Integrated structural approach to Credit Value Adjustment

Laura Ballotta[(a)], Gianluca Fusai[(a),(b)] and Daniele Marazzina[(c)]

[(a)]Faculty of Finance, Cass Business School, City, University of London

[(b)]Dipartimento SEI, Università del Piemonte Orientale, Novara, Italy

[(c)]Dipartimento di Matematica, Politecnico Milano, Italy

April 27, 2018

Abstract

This paper proposes an integrated pricing framework for Credit Value Adjustment of equity and commoditiy products. The given framework, in fact, generates dependence endogenously, allows for calibration and pricing to be based on the same numerical schemes (up to Monte Carlo simulation), and also allows the inclusion of risk mitigation clauses such as netting, collateral and initial margin provisions. The model is based on a structural approach which uses correlated Lévy processes with idiosyncratic and systematic components; the pricing numerical scheme, instead, efficiently combines Monte Carlo simulation and Fourier transform based methods. We illustrate the tractability of the proposed framework and the performance of the proposed numerical scheme by means of a case study on a portfolio of commodity swaps using real market data.

Keywords: Credit Value Adjustment, Collateral, Dependence, Gap Risk, Initial Margin, Lévy processes, Netting

JEL Classification: G13, G12, C63, D52

1 Introduction

In a post financial crisis landscape, the correct assessment and management of Counterparty Credit Risk (CCR) has become a core concern for both market regulators and financial institutions. The Basel III (Basel, 2010) supervisory regime in particular focuses on an enhanced sensitivity of credit risk measurement, as capital requirements have been linked to sophisticated measures of CCR such as Credit Valuation Adjustment (CVA), which acknowledges that during the last financial crisis two thirds of the losses due to CCR were caused by CVA market value changes (see BIS, 2011, for example). The financial crisis highlighted several aspects affecting CCR, such as dependence between default and exposures and risk mitigation, and the difficulties for market operators to take those consistently into account; for a detailed guide we refer to Brigo et al. (2013b); Gregory (2015) and references therein. Consequently, capital charges have been set up for mark-to-market losses associated with the deterioration of counterparty creditworthiness and any potential correlation with the contracts underlying financial asset (wrong-way risk).

In this paper we focus specifically on CVA originated by equity/commodity derivative contracts in presence of risk mitigation clauses. CVA calculation - which represents the first block towards

an integrated and comprehensive management of CCR - adds features of optionality and barrier conditions even to relatively standard contracts such as swaps and forwards; CVA, in fact, quantifies the so called expected positive exposure of the surviving financial entity, i.e. the positive value - if any - of the position under consideration which the survivor would lose in case of default of the counterparty. In this respect, the CVA shares strong similarity with a down-and-in call option, which is activated and settled only if one counterparty defaults and the other one survives. Thus, in general, the quantification of the above expectation is not immediate, as it requires a setting recognizing dependence between the default times of the two counterparties and the value of the overall position. Additional complexity stems from the presence of a number of important regulatory features, such as collateral agreements, netting provisions and initial margin. Indeed, in this case, the actual payoff is a package of calendar spread options on a basket, with additional barrier conditions capturing the triggering of the collateral agreements.

Our paper contributes to the current literature in a number of ways. Firstly, it offers an enhanced structural approach to credit modelling by considering driving risk processes with asymmetric and leptokurtic distributions. The choice of a setting based on the structural model is justified by the fact that it is the more natural framework for the pricing of equity-credit hybrid products and therefore for the quantification of CCR in equity products: indeed, as observed by Brigo et al. (2011) for example, the structural approach allows the introduction of dependence between the underlying and the counterparties in a natural way. This also facilitates significantly the calibration of the model, mainly due to the fact that dependence between firm values is reflected by dependence between equities. Furthermore, Brigo et al. (2011) report a stronger impact of wrong-way risk in a structural setting than with intensity models. The idea of non-Gaussian distributions stems instead from the need to properly portray 'extreme' events such as default, therefore improving the calibration performance of the structural approach (see Chen and Kou, 2009, for example). A structural approach for valuing corporate securities, seen as derivatives on a firms assets, and computing the term structure of both yield spreads and default probabilities has been proposed in Ayadi et al. (2016).

Secondly, our structural default model incorporates dependence between the counterparties and the underlying asset of the contract for which CCR is measured. This feature allows us to endogenously capture right/wrong-way risk, and quantify their impact on CVA in a straightforward manner. Although other constructions are possible, see for example the review offered in Itkin and Lipton (2015), in this work dependence is induced using the factor construction of Ballotta and Bonfiglioli (2016), so that the overall risk is decomposed into a systematic part and an idiosyncratic one. We observe that the factor model choice is in line with recommendations from the Basel Committee on Banking Supervision (Basel, 2013) for the development of internal models aimed at quantifying default risk charges. Further, factor constructions allow isolating dependence structure from the marginal distributions, which is an attractive feature from the practical point of view as market quotes of products required to calibrate the full correlation matrix might not be available due their lack of liquidity. Finally, as in the adopted factor construction dependence across entities is induced by a systematic source of risk, whilst the idiosyncratic components are independent, the complexity of the CVA pricing equation mentioned above can be significantly simplified by means of the conditional independence structure of the model. The general setup of the CVA problem is offered in Section 2,

whilst our framework is proposed in Section 3.

The third contribution offered by this paper is the development of a numerical scheme for the actual quantification of CVA, which is consistent and 'integrated' with the numerical scheme adopted for the actual model calibration. This is introduced in Section 4. The proposed method proves to be an efficient alternative to Monte Carlo (MC) simulation, i.e. the method of choice in practice. The complexity of the exposure in presence of mitigating clauses, the computation of default probabilities in a first-passage time setting, the presence of dependence rendering the default barriers both time and path dependent, significantly increase the computational cost associated with CVA measurement in a MC setting. In order to adequately capture all the above, MC needs to be extended through nested structures (see Pykhtin, 2011, for example). However, the proposed factor construction allows us to substitute nested Monte Carlo simulation with state of the art numerical schemes based on Hilbert transform (Feng and Linetsky, 2008) and Fourier cosine series (Fang and Oosterlee, 2008), speeding up considerably the computation of CVA.

Finally, by means of the developed framework, we explore issues of practical relevance, such as the effect of collateral agreements and initial margin in presence of right/wrong-way risk, and the quantification of gap risk under modelling assumptions able to generate tail dependence for typical values of correlation. We illustrate the point in Section 5 by means of a case study involving an energy sector company; the interest in this sector originates from the wave of credit ratings downgrades that has recently hit oil and gas companies (see Rodrigues and Crooks, 2015, for example). These market conditions have significantly affected energy prices, forcing oil companies to rethink their spending plans and squeezing high-cost producers (wrong-way risk) (see Noonan and McLannahan, 2015, as well).

We conclude this introduction with a brief reference to the literature closely related to the present topic. For exact Credit Default Swaps (CDS) calibration, CVA calculation and analysis of wrong-way risk impact in a structural setting, we refer to the already mentioned work of Brigo et al. (2011), who offer a framework based on a diffusion model, with either deterministic or stochastic barriers. Although both the approach in Brigo et al. (2011) and ours rely on the structural framework, our setting differs in the choice of the underlying risk processes. The flexibility of the underlying distribution offered by the general class of Lévy processes allows our model to reach the same calibration precision with less constraints on the overall dynamics of the model. Past work on pricing CCR for different asset classes, such as oil swaps, interest rate swaps and CDS can be found for example in Brigo and Bakkar (2009); Brigo et al. (2013a, 2014); the case of oil forwards in a simple setting à la Merton with no consideration for collateral agreements and initial margin can be found in Ballotta and Fusai (2015). We note that CVA for oil related products, to the best of our knowledge, has attracted little attention in the literature, in spite these being very common and natural products for which right/wrong-way risk effects can be observed. More recently, Brigo and Vrins (2018) have put forward a different approach to solve the computational issues caused by right/wrong-way risk for unilateral CVA in an intensity setting; this approach uses a set of equivalent measures named wrong way measures to 'remove' the dependence between the underlying asset and the counterparty default.

Unless otherwise stated, all proofs are deferred to the Appendix.

2 Preliminaries: CVA and first to default problem

In the following we consider a setting in which $S_1(t)$ and $S_2(t)$ represent the (risky) counterparties (i.e. the short and long position respectively) of derivative contract positions on reference names, denoted as $S_l(t)$, $l = 3, \cdots, n$, and with maturity T. At this stage we ignore default on the reference names, thus implicitly assuming that either their credit quality is stronger than the one of the counterparties, or the assets are non defaultable like, for example, an index or a commodity.

Let us further denote by τ_j the default time of counterparty $j = 1, 2$. Then, the bilateral CVA from the point of view of Firm 2 is defined as the present value of the expected loss in which Firm 2 incurs if Firm 1 defaults, Firm 2 survives at the moment in which the default of Firm 1 occurs, and the derivative positions on the reference names has a positive value to Firm 2, i.e.

$$CVA_1 = (1 - R_1)\mathbb{E}\left[1_{(\tau_1 \leq T)} 1_{(\tau_2 > \tau_1)} \Psi^+ (\tau_1; S_3, \ldots, S_n, T)\right], \tag{1}$$

where R_1 is the recovery rate on Firm 1 assets, $\Psi(t; S_3, \ldots, S_n, T)$ denotes the discounted value at time $t > 0$ of the derivative positions on $S_3, \ldots, S_n$ with maturity at time T, and $\Psi^+ = \max(\Psi, 0)$ denotes its positive part, i.e. the credit exposure to Firm 2. Alternative interpretations of the CVA (compared to the market value of the expected loss described above) include the cost of replacement of the counterparty in the given set of financial transactions (see Brigo et al., 2013b, for example), and more recently a fixed-point problem as in Kim and Leung (2016).

In our formulation (1), the CVA calculation takes into account the credit quality of both counterparties, also highlighting that the CVA materializes if the counterparty (in our case Firm 1) is the 'first to default'. This formulation of the bilateral CVA traces back to the 2008 preprint version of Brigo et al. (2012). The correction to the risk of counterparty default due to expected losses resulting from Firm 2 own default, i.e. Debt Valuation Adjustment (DVA) can be obtained following the same principle, as DVA is the CVA from the counterparty's perspective - see Brigo et al. (2012) for fuller details.

The quantification of CVA as defined in equation (1) requires a joint model for the entities $S_j(t)$, $j = 1, \ldots, n$, and the default event, which can conveniently accommodate for effects of right/wrong-way risk. A choice common in the literature is to cast the problem into the setting of the intensity approach to default risk, with dependence exogenously imposed via a suitably chosen copula (see also Crépey et al., 2014; Wu, 2015, for example). However, such a modelling choice poses in general non trivial problems in terms of model calibration and CVA calculation as the resulting joint distribution is not known in closed form. For a more detailed discussion concerning potential issues with intensity based models we refer to Brigo et al. (2013b) and references therein.

Consequently, in the following of this paper we adopt a setting based on the structural approach to default; however, due to the well known shortcomings of standard structural models based on diffusive dynamics, we enhance the setup by choosing Lévy processes as main risk drivers. The specific details of the model and the resulting setting are presented in the next section.

3 A Lévy-based structural model to default and CVA pricing

3.1 Lévy multivariate structural model for CVA

Consider a filtered probability space $(\Omega, \mathbb{F}, \{\mathbb{F}_t\}_{t\geq 0}, \mathbb{P})$, where $\mathbb{P}$ is a risk neutral martingale measure; a Lévy process $X(t)$ defined on this probability space is a continuous time process with independent and stationary increments, whose distribution has in general non-zero skewness and excess kurtosis, and is infinitely divisible. Hence, its characteristic function can be written as $\mathbb{E}\left(e^{iuX(t)}\right) = e^{t\varphi_X(u)}$ for any $u \in \mathbb{R}$; the function $\varphi_X(u)$ is the so-called characteristic exponent.

In this setting, we assume that the firm value of the j-th financial entity, $j = 1, \ldots, n$, is defined as

$$S_j(t) = S_j(0)e^{\left(r-q_j-\varphi_{X_j}(-i)\right)t+X_j(t)}, \quad j = 1, \ldots, n, \tag{2}$$

where $X_j(t)$ is a Lévy process with characteristic exponent $\varphi_{X_j}(\cdot)$, $r > 0$ is the continuously compounded risk-free rate[1], $q_j > 0$ is the constant cash flow pay out ratio, and n is the number of firms in the market. We note that in general the market is incomplete due to the fact that Lévy processes can accommodate jumps; consequently, we follow standard market practice and fix the pricing measure through calibration to the prices of suitably chosen traded derivative contracts.

Dependence between the risk drivers, $X_j(t)$, $j = 1, \ldots, n$, is modelled by the linear structure

$$\mathbf{X}(t) = \mathbf{Y}(t) + \mathbf{a}Z(t), \tag{3}$$

for $\mathbf{X}(t) = (X_1(t), ..., X_n(t))^\top$, $\mathbf{Y}(t) = (Y_1(t), ..., Y_n(t))^\top$, $\mathbf{a} = (a_1, ..., a_n)^\top \in \mathbb{R}^n$, and $Y_1(t), ..., Y_n(t)$ and $Z(t)$ mutually independent Lévy processes. Further, we assume that all relevant processes have finite moments of all orders; for full details see Ballotta and Bonfiglioli (2016); Ballotta et al. (2017).

In this framework default is modelled in the first passage time setting, in the sense that it is triggered at the first moment the firm value falls below an exogenous threshold, treated here as one of the model parameters. In addition, we make the realistic assumption that default is monitored at discrete dates, rather than continuously; this is consistent with industry practice which uses approximately weekly time steps in the first year to measure exposure with fine granularity at the short end, and quarterly in the following years (see Davidson, 2008, for example).

Thus, let us define the set $\mathcal{T} = (t_l)_{l=1}^{\mathcal{N}}$, then the default time τ is defined as the first time that the firm value S_j falls below a given level K_j, i.e.

$$\tau_j = \inf\{t \in \mathcal{T} : S_j(t) < K_j\} = \inf\{t \in \mathcal{T} : Y_j(t) + a_j Z(t) < l_j(t)\}, \tag{4}$$

where $l_j(t) = h_j - \hat{\mu}_j t$, for $h_j = \ln(K_j/S_j(0))$ and $\hat{\mu}_j = r - q_j - \varphi_{Xj}(-i)$. Here $t_{\mathcal{N}}$ denotes the expiry date of the firm's debt.

Although the use of factor models in the credit risk literature is not new (see, for example, the celebrated KMV model - Vašíček, 1987), our setup differs for its generality in terms of underlying distribution within the first passage time approach. Our model is, in fact, developed with respect to a

[1]For ease of illustration, we treat the rate of interest as constant; however, in the practical application it is time-dependent and suitably calibrated to the LIBOR curve (see Section 5.1 for further details).

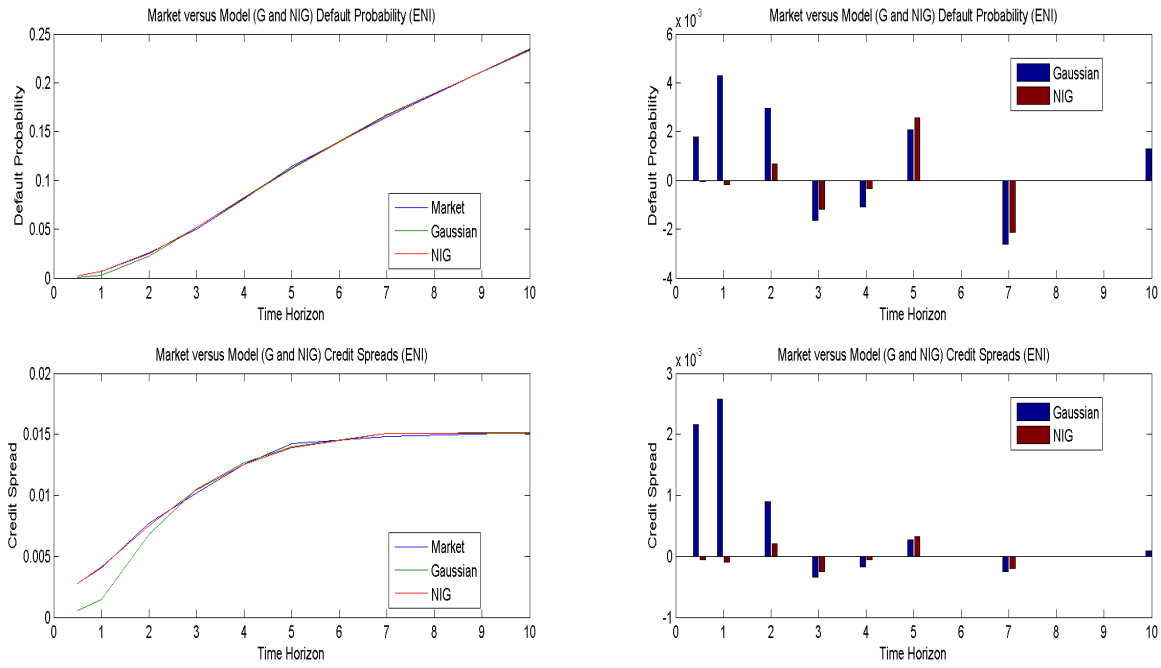

Figure 1: The importance of jumps: Gaussian (G) model vs NIG model. Top panels: probability of default (left-hand side); fitting error (right-hand side). Bottom panels: credit spreads (left-hand side); fitting error (right-hand side). Underlying asset: ENI. NIG model - parameter set: Table 3. Gaussian model - parameter set: $\sigma = 14.25\%$, $K = 0.01$.

generic Lévy process, and its implementation only requires the process to have a known characteristic function and finite moment of all orders. The early default feature does not introduce any particular computational difficulty as, by suitably conditioning, the CVA problem reduces to the well studied barrier option problem. Further, for calibration purposes we use credit spreads market quotes rather than generally unavailable balance sheet data. Detailed description and justification of the calibration procedure is deferred to Section 5.1.

In order to motivate the choice of a Lévy process as a driving process, we assess the improvements offered by a non-Gaussian structural model in capturing default probabilities and credit spreads compared to an equally calibrated structural model based on the Brownian motion (i.e. the traditional model of Black and Cox, 1976). This is shown in Figure 1, in which we plot the fitting errors of the two models calibrated to market credit spreads on a corporate firm (see Sections 4 - 5 for full details about the relevant modelling assumptions and the dataset). The most significant improvement is observable over the short period, i.e. for the case in which the traditional Gaussian-based model is known to perform poorly. This better performance of the Lévy process is due to its ability to capture, through the occurring of sudden jumps, changes in the firm rating over the short period, and the non zero credit spread.

In relation to solving the CVA problem (1), consistently with the assumptions set above, let us assume that the default event can only occur on a time grid $\{t_j : 0 \leq j \leq N\}$ for $t_0 = 0, t_N = T$; note that we assume, without loss of generality, that the contract expires before the firm's debt, i.e.

$t_N \leq t_{\mathcal{N}}$. Then

$$CVA_1 = (1 - R_1) \sum_{j=1}^{N} \mathbb{E}\left(1_{(t_{j-1} < \tau_1 \leq t_j)} 1_{(\tau_2 > t_j)} \Psi^+ \left(t_j; S_3, \ldots, S_n, T\right)\right). \tag{5}$$

Given the factor structure of the adopted model, it follows by conditioning on $\{Z(t), 0 < t \leq T\}$ that

$$CVA_1 = (1 - R_1) \sum_{j=1}^{N} \mathbb{E}\left[\mathbb{P}_Z\left(t_{j-1} < \tau_1 \leq t_j\right) \mathbb{P}_Z\left(\tau_2 > t_j\right) \mathbb{E}_Z\left(\Psi^+ \left(t_j; S_3, \ldots, S_n, T\right)\right)\right], \tag{6}$$

where $\mathbb{E}_Z(\cdot), \mathbb{P}_Z(\cdot)$ denote respectively the (risk neutral) conditional expectation and conditional probability with respect to the trajectory of the systematic risk process Z.

The computation of (6) requires on the one hand the exact definition of the exposure which depends on the payoff function of the contract under consideration - this is discussed in Section 3.2. On the other hand it also requires an efficient way of recovering the (conditional) default probabilities; this latter task is somewhat more straightforward as it uses standard techniques in barrier option pricing - the details of the actual implementation are delayed till Section 4.1.

3.2 The exposure: a general treatment - pricing exotic spread options

In order to present a complete argument, we assume the general case in which the transaction is covered by margin agreements aimed at limiting the potential exposure of one counterparty to another. Thus, in this setting, the function $\Psi^+(t; S, T)$ denotes the discounted value at time $t > 0$ of the so called collateralized exposure, $E_C(t)$, generated by a portfolio of derivative contracts on S_l, $l = 3, \cdots, n$, and maturity at time $T > t$, whose value at time $t > 0$ is $v(t, S_l)$. The t-value of the portfolio is then

$$\Pi(t) = \sum_{l=3}^{n} w_l v(t, S_l)$$

where $w_l, l = 3, \ldots, n$, are the quantities held in the portfolio of each derivative contract. Further, we also assume that netting agreements are allowed, on the basis of which, in the event of default of one of the counterparties, aggregation of transactions before settling is permitted. This is indeed the case in practice in presence of multiple trades within the same asset class and with the same counterparty (see Andersen et al., 2017, for example). Thus, netting represents a further risk mitigation mechanism as the values of all trades are added together, and therefore the resulting portfolio value is settled as a single trade[2] (see also Brigo and Masetti, 2006, for example). Under this set of assumptions, the collateralized exposure can be described as a package of calendar spread options written on a basket with some exotic features.

[2]According to ISDA (2010), netting benefit, measured as the difference between gross mark-to-market value and credit exposure after netting, was over 85% as of mid-2009. A similar measure for banks chartered in the United States was even greater, at about 90% of mark-to-market value.

To this purpose, let us consider the generic payoff

$$(A\Pi(t) - B\Pi(t-\delta t) + C - D\mathrm{IM}(t-\delta t))^{+}\, 1_{(E<\Pi(t-\delta t)<F)}, \tag{7}$$

with

A**:** the nominal size of the position considered which, without loss of generality, we assume 1.

B**:** the 'collateral' parameter originating the mark-to-market (MTM) value on which the so-called variation margin is calculated.

C**:** the threshold determining the amount of variation margin which parties are required to post; it should be considered as the excess which, if surpassed by the MTM, determines the incremental amount called for.

D**:** the 'initial margin' parameter, controlling whether or not this form of collateral is to be accounted for in the CVA calculation; the initial margin is denoted as IM.

E, F**:** thresholds triggering the call of the variation margin for the two counterparties; they usually coincide with the excess threshold C augmented by an amount, $M > 0$, representing the so called minimum transfer amount (MTA).

In the following we provide some insights regarding the structure (7) in the context of CVA determination. For fuller details we refer the interested readers to Bielecki et al. (2011); Gregory (2015) for example. The calculation of the exposure generated by any position should take into account the appreciation/depreciation of the position value as this determines the actual loss for the surviving counterparty in case of default of the other one. Risk mitigation clauses aimed at reducing this exposure are provided by the so-called collateral agreements, based on which either counterparty is required to post collateral against a negative (from their point of view) MTM value.

As hinted above, two types of collateral are usually identified: the variation margin and the initial margin. The variation margin is collateral reflecting the MTM of the transaction; it is calculated as the incremental amount of the MTM value compared to the excess C. The mechanism can be described in general terms as follows. Let $t - \delta t$ be the date at which the last collateral has been posted before the next monitoring date $t > 0$. If at $t - \delta t$ the MTM is positive, i.e. $\Pi(t - \delta t) > 0$, then Firm 2, who holds the long position in the portfolio, stands to face losses in case Firm 1 defaults in $(t - \delta t, t]$. Thus Firm 2 calls for collateral in excess of $C = H_1 > 0$ to be posted by Firm 1, if the MTM exceeds the triggering threshold $H_1 + M$. Consequently, the exposure of Firm 2 at t will be given by the current MTM value, $\Pi(t)$, cleared of any collateral posted by Firm 1 at $t-\delta t$. Viceversa, if at $t - \delta t$ the MTM is negative, i.e. $\Pi(t - \delta t) < 0$, it is Firm 1 which stands to suffer losses in case of default of Firm 2, and therefore calls for collateral in excess of $C = H_2 < 0$, provided the MTM exceeds the triggering threshold $H_2 - M$. The quantity M, representing the MTA, is an additional clause aimed at reducing the collateral frequency of exchange, due to the expensive nature of this operation for the counterparties. We note that throughout the paper collateral is defined as cash

amount which does not earn any interest[3].

The second form of collateral in place is the initial margin, IM. This is an amount of additional buffer which both counterparties are required to post irrespectively of the MTM value of the underlying position. Because of this, the initial margin can be considered as the first line of defence for risk mitigation. For these reasons, its calculation should be based on extreme, but plausible, movements in the underlying position MTM at a $p = 99\%$ confidence level as measured by the Value at Risk (VaR). For a portfolio of derivative contracts, the VaR is equivalent to

$$\mathrm{IM}(t-\delta t) = \Pi(t-\delta t) - \Pi^{p}(\Pi(t-\delta t+\Delta t))$$

where $\Pi^{p}(\cdot)$ denotes the worst case scenario (i.e. the quantile of the distribution) of the position at a $(1-p)\%$ confidence level, expressed as a function of the portfolio value, over a Δt-day time horizon (usually 10 days).

Based on the general description given above, the collateralized exposure with initial margin for Firm 2 at time t is

$$\begin{aligned} E_C(t) = &\left(\Pi(t) - \mathrm{IM}(t-\delta t)\right)^{+} 1_{(H_2-M \le \Pi(t-\delta t) \le H_1+M)} && \text{(8a)} \\ &+ \left(\Pi(t) - \Pi(t-\delta t) + H_1 - \mathrm{IM}(t-\delta t)\right)^{+} 1_{(\Pi(t-\delta t) > H_1+M)} && \text{(8b)} \\ &+ \left(\Pi(t) - \Pi(t-\delta t) + H_2 - \mathrm{IM}(t-\delta t)\right)^{+} 1_{(\Pi(t-\delta t) < H_2-M)}. && \text{(8c)} \end{aligned}$$

In detail $E_C(t)$ is decomposed in three components that can be reconducted to the general payoff (7). The term (8a) in the above represents the 'uncollateralized' exposure (up to the initial margin) which originates from the MTM at $t-\delta t$ not exceeding any of the triggering thresholds. The second term (8b) is the exposure after the collateral is called by Firm 2 and posted by Firm 1; the final term (8c) originates instead in the opposite situation in which the collateral is called by Firm 1 and posted by Firm 2. Each term corresponds to (7) for the parameter settings given in Table 1, which also reports the setting for the case of the 'crude' exposure, and the collateralized exposure under unilateral agreement. Finally, we note that this general formulation of the exposure corresponds broadly to the 'classical model' of Andersen et al. (2017).

The above shows that the actual calculation of the expected (discounted) exposure

$$\mathbb{E}_Z\left(\Psi^{+}\left(t_j; S_3, \ldots, S_n, T\right)\right) \tag{9}$$

in (6), can be reduced to the calculation of the expectation of the discounted payoff (7), based on the corresponding contract setting. Bearing in mind that we condition on the trajectory of the systematic process $Z(t)$, the task of obtaining (9) can be further simplified by also conditioning on the information available at time $t-\delta t$. However, the actual solution of (9) depends on the specification of the contract payoff function; in this work we focus on the case of linear derivatives such as swaps

[3]According to ISDA (2014, 2015a), estimated collateral for non-cleared OTC derivatives is around $3.2 trillions at the end of 2013; there is small decline over the last few years due in part to a continued shift to central clearing. Indeed, 90% of all OTC derivatives was subject to collateral agreement at the end of 2013. Cash and government securities account for 90% of non-cleared OTC derivatives collateral.

	Payoff	A	B	C	D	E	F
Uncollateralized Exposure		1	0	0	1	$E \to -\infty$	$F \to \infty$
Unilateral	eq. (8a)	1	0	0	1	$E \to -\infty$	$H_1 + M$
Collateralized	eq. (8b)	1	1	H_1	1	$H_1 + M$	$F \to \infty$
Exposure	eq. (8c)	–	–	–	–	$E \to -\infty$	$F \to -\infty$
Bilateral	eq. (8a)	1	0	0	1	$H_2 - M$	$H_1 + M$
Collateralized	eq. (8b)	1	1	H_1	1	$H_1 + M$	$F \to \infty$
Exposure	eq. (8c)	1	1	H_2	1	$E \to -\infty$	$H_2 - M$

Table 1: Parameter setting of payoff (7) when modelling collateralized exposure in eq. (8a) - eq. (8c). Note. If the initial margin is not applied, $D = 0$.

and forwards (which are a particular case of swaps) on equity and commodity as illustrated in the following sections.

3.3 Swap contracts: single trade

Assume a single swap contract on S_3, with maturity T, payments dates $T_1, T_2, ..., T_{N_S} = T$ and swap rate K_3 (as previously observed, if $N_S = 1$, the swap reduces to a forward contract). Then

$$v(t, S_3) = \sum_{j:T_j>t} \left(S_3(t)\, e^{-q_3(T_j-t)} - K_3 e^{-r(T_j-t)} \right) \tag{10}$$

and $\Pi(t) = v(t, S_3)$. In this case the solution to (9) simplifies significantly. Due to the factor structure of the driving process, in fact, (10) can be written as

$$v(t, S_3) = \alpha_3(t)\beta(t; a_3 Z) S_3(0) e^{(r-q_3-\varphi_{Y_3}(-i))t+Y_3(t)} - \bar{K}_3(t), \tag{11}$$

$\alpha_3(t) = \sum_{j:T_j>t} e^{-q_3(T_j-t)}$, $\beta(t; a_3 Z) = e^{-\varphi_Z(-a_3 i)t + a_3 Z(t)}$ and $\bar{K}_3(t) = K_3 \sum_{j:T_j>t} e^{-r(T_j-t)}$. Hence, the pricing of the collateralized exposure can be linked directly to the idiosyncratic component Y_3.

For what concerns the initial margin, in this simplified setting the worst case scenario $\Pi^p(\cdot)$ reduces to a monotonic function of the position at the last monitoring date $t - \delta t$ and the worst increment of the margin process X_3 over the monitoring period Δt. As the increments of Lévy processes are independent, we can compute the quantile $X_3^p(\Delta t)$ of these increments separately from the rest.

Under the assumptions leading to the CVA equation (6), specifically by conditioning on the trajectory of the systematic process $Z(t)$, the following result holds for (9).

Proposition 1 *The market consistent value (9) for $\Pi(t) = v(t, S_3)$ and $v(t, S_3)$ given by (11) has expression*

$$\alpha_3(t)\beta(t; a_3 Z) \int_{LB}^{UB} \mathbb{E}_Z \left(e^{-rt} \left(AG(t-\delta t; y) e^{(r-q_3-\varphi_{Y_3}(-i))\delta t + (Y_3(t)-y)} - \tilde{K}(y) \right)^+ \right) f_{Y_3(t-\delta t)}(y) dy,$$

with $f_{Y_3(t)}(\cdot)$ denoting the probability density function of the idiosyncratic process $Y_3(t)$,

$$
\begin{aligned}
&G(t;Y_3) = S_3(0)e^{(r-q_3-\varphi_{Y_3}(-i))t+Y_3(t)},\\
&\tilde{K}(Y_3) = \frac{1}{\alpha_3(t)\beta(t;a_3Z)}\left[A\bar{K}_3(t) - (B+D)\bar{K}_3(t-\delta t) + D\bar{K}_3(t-\delta t+\Delta t) - C\right.\\
&\qquad\left. -\beta(t-\delta t;a_3Z)G(t-\delta t;Y_3)\left(D\alpha_3(t-\delta t+\Delta t)e^{\left(r-q_3-\varphi_{X_3}(-i)\right)\Delta t+X_3^p(\Delta t)} - (B+D)\alpha_3(t-\delta t)\right)\right],\\
&LB = \ln\left(\frac{E+\bar{K}_3(t-\delta t)}{\alpha_3(t-\delta t)\beta(t-\delta t;a_3Z)S_3(0)}\right) - (r-q_3-\varphi_{Y_3}(-i))(t-\delta t),\\
&UB = \ln\left(\frac{F+\bar{K}_3(t-\delta t)}{\alpha_3(t-\delta t)\beta(t-\delta t;a_3Z)S_3(0)}\right) - (r-q_3-\varphi_{Y_3}(-i))(t-\delta t),
\end{aligned}
$$

and $X_3^p(\Delta t)$ denoting the worst case scenario (quantile) at $(1-p)\%$ confidence level of the process X_3 over a Δt-day time horizon. We set $LB \to -\infty$ if $E+\bar{K}_3(t-\delta t) \leq 0$.

From the practical point of view, the pricing equation in Proposition 1 can be solved firstly by computing the inner conditional expectation, and secondly by performing (numerical) integration with respect to the density function of the Lévy process Y_3 of choice. As the inner conditional expectation corresponds to the price of a plain vanilla European call option, pricing can be achieved by a suitably chosen Fourier inversion method. The quantile $X_3^p(\Delta t)$ is computed by (numerical) inversion of the distribution function of X_3. Further details are provided in Section 4.1.

We notice that in case of restrictions on netting agreements, the expected exposure of a portfolio of derivative contracts is the sum of each single expected collateralized exposure as given, for the example of swaps, in Proposition 1.

As documented for example by Brigo et al. (2014), although in presence of collateral agreements, counterparties are required to periodically mark to market their positions, these risk mitigation clauses do not completely eliminate counterparty credit risk, as sudden movements can increase both the exposure since the time of the last collateral exchange, and the probability of the relevant default event. This originates the so called gap risk and gap event, which is the event in which at time $t > 0$ the counterparty, $S_1(t)$, defaults, the investor, $S_2(t)$, survives and the contract on the underlying asset, $S_3(t)$, moves in the money, given that at time $t-\delta t$, the counterparty was solvent and the exposure was either out-of-the money or perfectly collateralized. In the proposed structural model, the probability of this event (seen from the point of view of Firm 2) can be written as

$$
P_{Gap} = \mathbb{P}\left(S_1(t) < K_1, S_2(t) \geq K_2, v(t,S_3) > 0 \middle| S_1(t-\delta t) \geq K_1, S_2(t-\delta t) \geq K_2, v(t-\delta t,S_3) \leq 0\right). \tag{12}
$$

As the collateral posting is by regulation operated with high frequency, (12) expresses a measure of extreme co-movement of the three random quantities involved over a very short period, i.e. it is a measure of tail dependence for the joint distribution of the three risk drivers (see McNeil et al., 2015, for example, for more details on tail dependence). This observation leads us to the following considerations. Firstly, in the structural framework, gap risk can only be properly generated if the joint sources of risk have sufficient probability mass in the tails. This rules out the Gaussian distribution due to the very fast decay rate of its tails (see Embrechts et al., 2002, for example). Lévy processes, other than the Brownian motion, can cater for slower decay rate of the distribution tails, offering the possibility of a more realistic quantification of the probability of a gap event. Secondly,

the initial margin has become a compulsory regulatory element aimed at precisely reducing gap risk; indeed, in presence of initial margin in (12), the value of the contract would have to exceed the actual value of the initial margin for the gap event to be triggered. Finally, our factor construction (3) allows for a straightforward way of obtaining (12) in closed form by using the same argument as in Oh and Patton (2017), i.e. the probability of sums of random variables all exceeding some diverging threshold is driven completely by the common component of the sums. In the interest of readability, we offer the analytical result in the Appendix.

3.4 Swap contract: portfolio of trades

In this case

$$\Pi(t) = \sum_{l=3}^{n} w_l \left(\alpha_l(t)\beta(t; a_3 Z) S_l(0) e^{(r-q_l-\varphi_{Y_l}(-i))t+Y_l(t)} - \bar{K}_l(t) \right); \tag{13}$$

then, the solution of the general pricing equation (9) is more complex due mainly to two reasons. The first reason is the calculation of the worst case scenario for the portfolio, i.e. Π^p. Given the independent increments of Lévy processes, this issue is resolved by obtaining the increments of the relevant margin processes over the monitoring period Δt at the start of the computation procedure and then considering them as fixed. This implies that the portfolio's worst case scenario can be considered as a function of the portfolio value at the last reset date and the monitoring period, i.e. $\Pi^p(\Pi(t-\delta t), \Delta t)$.

The second reason is the lack of analytical form for the density function of a basket of exponential Lévy processes. This latter issue can be tackled by means of a bivariate Edgeworth expansions (see Polley, 2016, for example, and references therein). This approach is justified by the fact that, conditioned on the trajectory of the systematic risk process Z, the portfolio value is determined by a sum of independent exponential Lévy process, as highlighted by (13).

To the purpose of the application of Edgeworth expansion, we require some preliminary definitions and results. Let $\boldsymbol{\alpha} = (\alpha_1, \alpha_2)$ be a multi-index, i.e. pair of non-negative integers, and define $|\boldsymbol{\alpha}| = \alpha_1 + \alpha_2$, $\boldsymbol{\alpha}! = \alpha_1!\alpha_2!$ and $x^{\boldsymbol{\alpha}} = x_1^{\alpha_1} x_2^{\alpha_2}$ for $x \in \mathbb{R}^2$. Further, let

$$f_{N,\Sigma}(\xi) = \frac{1}{2\pi\sqrt{1-\rho^2}} e^{-\frac{\xi_1^2 - 2\rho\xi_1\xi_2 + \xi_2^2}{2(1-\rho^2)}}$$

be the bivariate standard normal distribution. Finally, we define the 2-dimensional Hermite polynomials as

$$H_{\boldsymbol{\alpha}}\left(\xi, \Sigma^{-1}\right) = (-1)^{\boldsymbol{\alpha}} f_{N,\Sigma}(\xi)^{-1} \frac{\partial^{|\boldsymbol{\alpha}|}}{\partial\xi_1^{\alpha_1}\partial\xi_2^{\alpha_2}} f_{N,\Sigma}(\xi).$$

The explicit expression of these polynomials up to order six is given in Barndorff-Nielsen and Pedersen (1979).

Consider the bivariate process $(\Pi(t), \Pi(t-\delta t))$ and let us denote $m_1 = \mathbb{E}_Z(\Pi(t))$, $m_2 = \mathbb{E}_Z(\Pi(t-\delta t))$, $\sigma_1^2 = \mathbb{V}ar_Z(\Pi(t))$, $\sigma_2^2 = \mathbb{V}ar_Z(\Pi(t-\delta t))$, $\sigma_{12} = \mathbb{C}ov_Z(\Pi(t-\delta t), \Pi(t))$. Let $\xi_1 = (\Pi(t) - m_1)/\sigma_1, \xi_2 = (\Pi(t-\delta t) - m_2)/\sigma_2$ be the standardized versions of the values of the portfolio (for

ease of notation we suppress dependence on time of all relevant quantities). Then the Edgeworth expansion of the joint density of $\xi = (\xi_1, \xi_2)$ is

$$f_\xi(\xi) = f_{N,\Sigma}(\xi)\left(1 + \sum_{|\boldsymbol{\alpha}|=3}^{\infty} \frac{K_\xi^{\boldsymbol{\alpha}}}{\boldsymbol{\alpha}!} H_{\boldsymbol{\alpha}}\left(\xi, \Sigma^{-1}\right)\right), \tag{14}$$

with $K_\xi^{\boldsymbol{\alpha}}$ denoting the co-cumulant of order $\boldsymbol{\alpha}$ of $\xi = (\xi_1, \xi_2)$, i.e.

$$K_\xi^{\boldsymbol{\alpha}} = K_\xi^{(\alpha_1,\alpha_2)} = (-i)^{|\boldsymbol{\alpha}|} \left.\frac{\partial^{|\boldsymbol{\alpha}|}}{\partial u_1^{\alpha_1} \partial u_2^{\alpha_2}} \ln \mathbb{E}(e^{iu_1\xi_1 + iu_2\xi_2})\right|_{u_1=0, u_2=0}.$$

For practical purposes we truncate the summation in (14) to $|\boldsymbol{\alpha}| = 4$, so that (14) reduces to the bivariate version of the so-called Gram-Charlier A expansion (see Mardia, 1970, for example).

In virtue of the properties of the bivariate normal distribution and the nature of the 2-dimensional Hermite polynomials, the following holds.

Proposition 2 *The market consistent value (9) for the general portfolio* $\Pi(t) = \sum_{l=3}^{n} w_l v(t, S_l)$ *and* $v(t, S_l)$ *given by (11)), under the Gram-Charlier A approximation, has expression*

$$e^{-rt}\int_E^F g(y)dy + e^{-rt}\sum_{|\boldsymbol{\alpha}|=3}^{4} \frac{1}{\boldsymbol{\alpha}!}\frac{K_{\boldsymbol{\Pi}}^{\boldsymbol{\alpha}}}{\boldsymbol{\sigma}^{\boldsymbol{\alpha}}} \sum_{i,j=0}^{|\boldsymbol{\alpha}|} h_{i,j}^{\boldsymbol{\alpha}} \int_E^F g_i(y)\left(\frac{y - m_2}{\sigma_2}\right)^j dy,$$

for

$$\begin{aligned}
g(y) &= \frac{1}{\sigma_2\sqrt{2\pi}} e^{-\frac{(y-m_2)^2}{2\sigma_2^2}} \left(A\frac{\sigma_{1|2}}{\sqrt{2\pi}} e^{-\frac{1}{2}d(y)^2} + \left(Am_{1|2}(y) - (B+D)y + C + D\Pi^p(y,\Delta t)\right)\mathcal{N}\left(d(y)\right)\right), \\
g_i(y) &= \frac{1}{\sigma_2\sqrt{2\pi}} e^{-\frac{(y-m_2)^2}{2\sigma_2^2}} \left(A\sigma_1\bar{m}_{i+1}(y) + \left(Am_1 - (B+D)y + C + D\Pi^p(y,\Delta t)\right)\bar{m}_i(y)\right), \\
\bar{m}_k(y) &= \frac{\sigma_{12}}{\sigma_1\sigma_2}\left(\frac{y-m_2}{\sigma_2}\right)\bar{m}_{k-1}(y) + (k-1)\frac{\sigma_{1|2}^2}{\sigma_1^2}\bar{m}_{k-2}(y) \\
&\quad + \frac{\sigma_{1|2}}{\sigma_1}\left(-\frac{Am_1 - (B+D)y + C + D\Pi^p(y,\Delta t)}{A\sigma_1}\right)^{k-1} \frac{1}{\sqrt{2\pi}} e^{-\frac{d(y)^2}{2}}, \\
\bar{m}_0(y) &= \mathcal{N}\left(d(y)\right), \qquad \bar{m}_{-1}(y) = 0, \\
d(y) &= \frac{m_{1|2}(y) - (B+D)y/A + (C + D\Pi^p(y,\Delta t))/A}{\sigma_{1|2}}, \\
m_{1|2}(y) &= m_1 + \frac{\sigma_{12}}{\sigma_2^2}(y - m_2), \qquad \sigma_{1|2}^2 = \sigma_1^2 - \frac{\sigma_{12}^2}{\sigma_2^2},
\end{aligned}$$

$\mathcal{N}(\cdot)$ *denotes the standard normal cumulative distribution function,* $\boldsymbol{\sigma} = (\sigma_1, \sigma_2)$*,* $K_{\boldsymbol{\Pi}}^{\boldsymbol{\alpha}}$ *denotes the co-cumulant of* $(\Pi(t), \Pi(t - \delta t))$ *of order* $\boldsymbol{\alpha}$*, and* $h_{i,j}^{\boldsymbol{\alpha}}$ *denotes the* ij *coefficient of the terms* $\xi_1^i\xi_2^j$ *in the 2-dimensional Hermite polynomial of order* $\boldsymbol{\alpha}$*.*

We note that in the case of equally weighted and homogeneous portfolio of swaps, i.e. for which

$w_l = 1/(n-2)$, $a_l = a_3$, $l = 3, \cdots, n$, and $Y_l(t)$ are independent copies of the idiosyncratic process $Y_3(t)$, the following holds.

Corollary 3 *The market consistent value (9) for an equally weighted large portfolio of swaps with value function (11) on homogeneous assets has expression*

$$e^{-rt}\int_E^F \frac{1}{\sigma_2\sqrt{2\pi}} e^{-\frac{(y-m_2)^2}{2\sigma_2^2}} \left(A\frac{\sigma_{1|2}}{\sqrt{2\pi}} e^{-\frac{1}{2}d(y)^2} + \left(Am_{1|2}(y) - (B+D)y + C + D\Pi^p(y,\Delta t)\right)\mathcal{N}\left(d(y)\right)\right) dy + o(n^{-1/2}).$$

We conclude this section by noting that the 'crude' CVA without any collateral agreement can be recovered from the previous results by setting $B = C = D = 0$, $E \downarrow -\infty$, $F \uparrow \infty$. In the interest of space, the full argument is provided in the Appendix.

4 Numerical implementation and testing

This section discusses the numerical computation of the quantities appearing in the CVA equation (6), based on the model features and the exposure functions introduced in Section 3. For the purpose of the numerical analysis, we choose as a relevant Lévy process the Normal Inverse Gaussian (NIG) process introduced by Barndorff-Nielsen (1995). In more details, the NIG process is a normal tempered stable process obtained by subordinating a Brownian motion by an (unbiased) independent Inverse Gaussian process. Its characteristic exponent reads

$$\varphi_X(u) = \frac{1}{k}(1 - \sqrt{1 - 2iu\theta k + u^2\sigma^2 k}), \quad u \in \mathbb{R}.$$

It follows that the first four cumulants of the process are $K^{(1)} = \theta t$, $K^{(2)} = \left(\sigma^2 + \theta^2 k\right) t$, $K^{(3)} = 3\theta k \left(\sigma^2 + \theta^2 k\right) t$, and $K^{(4)} = 3k\left(\sigma^4 + 6\sigma^2\theta^2 k + 5\theta^4 k^2\right) t$. Hence, $\theta \in \mathbb{R}$ controls the sign of the skewness of the process distribution, $\sigma > 0$ affects the overall variability and $k > 0$ controls the kurtosis of the distribution. Moreover, the tails of the distribution are characterized by a power-modified exponential decay, or semi-heavy tail (see Cont and Tankov, 2004, for example).

All numerical experiments refer to swap contracts with 1 year maturity and weekly payment dates ($N_S = 52$), which we assume to coincide with the default monitoring dates (i.e. $N = N_S$). The model parameters are obtained through calibration as described in details in Section 5.1 and reported in Table 3. The numerical schemes are implemented in MATLAB R2015A and run on a computer with an Intel i7-3.20GHz CPU, and 4GB of RAM.

4.1 Implementation

'Outer Analytics'. Monte Carlo

We recall that the pricing equations obtained in Section 3 have been derived by conditioning first on the trajectory of the systematic process Z, in order to exploit the properties of the factor model adopted in this paper. This paves the way for MC simulation applied to the outer expectation of (6). To this purpose, we assume that the points on the time grid $\{t_j : 0 \le j \le N\}$ for $t_0 = 0$, $t_N = T$, are

equally spaced so that $t_j = t_0 + j\delta$, $j = 1, \ldots, N$ with $\delta = T/N$. Then (6) is computed as

$$(1 - R_1) \sum_{j=1}^{N} \frac{1}{M_C} \sum_{m=1}^{M_C} \mathbb{P}_{Z^{(m)}} \left((j-1)\delta < \tau_1 \leq j\delta \right) \mathbb{P}_{Z^{(m)}} \left(\tau_2 > j\delta \right) \mathbb{E}_{Z^{(m)}} \left(\Psi^+ \left(j\delta; S_3, T \right) \right), \tag{15}$$

where M_C is the total number of simulations trials, and $Z^{(m)}$, $m = 1, \ldots, M_C$, is the m-th simulated path of the process $Z(t)$. Efficient MC algorithms for the NIG process can be based on its representation as subordinated Brownian motion as detailed in Cont and Tankov (2004).

'Inner Analytics'. Default probabilities

Given the assumptions above and the setting of Section 3.1, the conditional (risk neutral) probabilities in (15) refer to a conditional default time

$$\tau^{(m)} = \inf \left\{ t \in \mathcal{T} : Y(t) < l(t) - aZ^{(m)}(t) \right\}, \quad m = 1, \ldots, M_C,$$

for $\mathcal{T} = \delta, \ldots, j\delta, \ldots, N\delta = T$ (for ease of exposition, we suppress the firm specific index).

The most intuitive approach to the computation of the given probabilities would be MC simulation again, which would be in this case nested in the MC simulation of the systematic process Z - hence, we label this method as FullMC(k), where $k \in \mathbb{N}$ denotes the number of nested simulation trials for the trajectory of Y, per each trajectory of Z (FullMC(10^0) denotes the classical unnested MC). However, due to both the time and path dependent barrier defining the default event, we expect the FullMC(k) method to be particularly time consuming for any desired level of accuracy, as it would require $M_C \times k$ simulation trials.

As alternative we consider the Hilbert transform method of Feng and Linetsky (2008). This choice is motivated by the similarity of the computational problem of the survival probabilities with the pricing of discretely monitored barrier options; further, the method shows a computational cost of order $\mathcal{O}(NP \log P)$, for N the number of monitoring dates and P the number of grid points, and exponentially decaying error. This makes the approach superior to other Fourier transform based methods (see Feng and Linetsky, 2008, and references therein for further details). More precisely, we apply the Hilbert method to compute the survival probability via the following recursion: let $p^{(m)}(x, j)$ be the probability that $Y(j\delta) = x$ given that the lower barrier $b^{(m)}(t) = l(t) - aZ^{(m)}(t)$ has never been touched by the process Y in $t = \{\delta, 2\delta, \cdots, j\delta\}$. Then, $p^{(m)}(x, 0)$ is the Dirac delta function centered in $Y(0) = 0$, and it holds

$$p^{(m)}(x, j) = \int_{-\infty}^{\infty} f(x - x', \delta) p^{(m)}(x', j-1) dx' \; 1_{(x \geq b^{(m)}(j\delta))}, \quad j = 1, \cdots, N, \tag{16}$$

where f is the probability density function of the Lévy process Y. The survival probability in $j\delta$ is therefore given by

$$\mathbb{P}_{Z^{(m)}} \left(\tau > j\delta \right) = \int_{-\infty}^{\infty} p^{(m)}(x, j) dx.$$

We label this method as MC+Hilbert(P).

'Inner Analytics'. Expected exposures

For ease of computation, but without loss of generality, we assume that the margining dates coincide with the time points on the partition $\{t_j : 0 \leq j \leq N\}$ for $t_0 = 0, t_N = T$. As far as the length of the margining period is concerned, it depends on the frequency with which the collateral is re-adjusted; in the following we assume for illustrative purposes and without loss of generality $\delta t = \delta$, i.e. 1 week[4]. Thus, in the case of Proposition 1, we choose the COS method introduced by Fang and Oosterlee (2008) for the efficient computation of both the European vanilla options and the density function of Y_3, exploiting its exponential accuracy in the number of grid points. Hence, for fixed value of $Y_3(t-\delta t)$, we first obtain the conditional values by means of the COS method, then, we integrate with respect to the density function of $Y_3(t-\delta t)$, using the QUAD routine in MATLAB. In the case of Proposition 2, due to the analytical nature of the integrand functions, we only require the numerical integration part.

In both cases, though, the full collateralized exposure is a package of basket options with prices as in Propositions 1 and 2. Therefore, in order to speed-up the MC+Hilbert algorithm, we pre-compute the values of the integrals on a two-dimensional array and use these values to interpolate the required quantities. In practice, given a simulated path of the common factor, at each time step t, we proceed as follows.

- Construct a grid of $\widehat{M}$ points $Z_j^- = \min_{m=1,\cdots,M} Z^{(m)}(t-\delta t) + j\widehat{\Delta}$, $j = 0, \cdots \widehat{M}-1$, with $\widehat{\Delta} = \frac{1}{\widehat{M}-1}\left(\max_{m=1,\cdots,M} Z^{(m)}(t-\delta t) - \min_{m=1,\cdots,M} Z^{(m)}(t-\delta t)\right)$.
- Construct a grid of $\widehat{M}$ points $Z_j^+ = \min_{m=1,\cdots,M} Z^{(m)}(t) + j\widehat{\Delta}$, $j = 0, \cdots \widehat{M}-1$, with $\widehat{\Delta} = \frac{1}{\widehat{M}-1}\left(\max_{m=1,\cdots,M} Z^{(m)}(t) - \min_{m=1,\cdots,M} Z^{(m)}(t)\right)$.
- Compute the integrals in both Proposition 1 and 2 on the bidimensional array of Z.
- For each simulated trajectory $Z^{(m)}$, evaluate the expected exposure via linear interpolation on the bidimensional grid $(Z^{(m)}(t-\delta t),\, Z^{(m)}(t))$.

Finally, with reference to Proposition 2, under the assumption of equally weighted and homogeneous portfolio, the worst case scenario of the portfolio is

$$\begin{aligned}\Pi^p(\Pi(t-\delta t), \Delta t) &= \alpha_3(t-\delta t+\Delta t)\beta(t-\delta t; a_3 Z) S_3(0) e^{(r-q_3-\varphi_{Y_3}(-i))(t-\delta t)} \mathcal{Y}(t-\delta t) e^{(r-q_3-\varphi_{X_3}(-i))\Delta t} \mathcal{X}^p(\Delta t) \\ &- \bar{K}_3(t-\delta t+\Delta t),\end{aligned}$$

for

$$\mathcal{Y} = \frac{1}{n-2}\sum_{l=3}^{n} e^{Y_l}, \qquad \mathcal{X} = \frac{1}{n-2}\sum_{l=3}^{n} e^{Y_l + a_l Z}, \tag{17}$$

and $\mathcal{X}^p(\Delta t)$ is the worst case scenario at $(1-p)\%$ confidence level of the process $\mathcal{X}$ over a Δt time horizon. $\mathcal{X}^p$ can be easily computed once the distribution of $\mathcal{X}$ is known. This can be achieved by first

[4]It is worth, for reason of clarity, pointing out the different time periods entering the computation of CVA and related quantities: δt denotes the length of the margining period, i.e. the frequency with which the collateral is readjusted; δ is the length of the default monitoring period, i.e. the frequency with which the survival of the companies entering the given transaction is monitored; finally Δt is the VaR time horizon for the IM computation, set to 2 weeks (10 working days). In general, $\delta t, \delta, \Delta t$ are different and depend on contracts clauses and supervisory requirements.

Method	CPU	$\mathbb{P}_{S_1}$	s.e.	CVA (bps)	s.e. (bps)	CPU
FullMC(10^0)	85	0.707340	0.001838	829.39	9.04	92
FullMC(10^1)	699	0.706736	0.001278	818.38	2.96	711
FullMC(10^2)	965	0.706867	0.001261	822.20	1.36	976
FullMC(10^3)	1799	0.706811	0.001259	820.12	1.07	1831
FullMC(10^4)	10525	0.706792	0.001259	820.17	1.03	10541
MC+Hilbert(2^9)	286	0.706865	0.001259	819.83	1.03	295
MC+Hilbert(2^{10})	632	0.706795	0.001259	820.05	1.04	645

Table 2: FullMC vs Hybrid Method: Testing. CVA (in bps), survival probabilities of S_1 ($\mathbb{P}_{S_1}$) at time $t = 0.5$ (six months), and execution time (in seconds). Parameters: Table 3. Other parameters: $S_1(0) = S_2(0) = S_3(0) = 1$, $T = 1$ year; weekly monitoring. FullMC(k): Monte Carlo with k simulations for each trajectory of Z. MC+Hilbert(P): Hilbert method implemented with P grid points. $M_C = 10^5$ simulation trials. CVA computation: (conditional) expected exposure computed using the COS method with 2^9 grid points and truncation range set for $L = 15$.

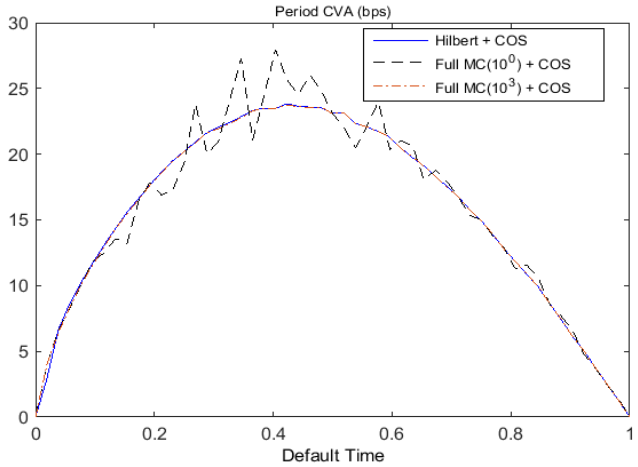

Figure 2: Computation of the CVA comparing Full Monte Carlo and Hybrid Method. FullMC(k): Monte Carlo with k simulation trials for each trajectory of the systematic process Z; $M_C = 10^5$ simulation trials. Hilbert and COS methods: $P = 2^9$ grid points, $L = 15$. Parameter set: Table 3. Other parameters: $S_1(0) = S_2(0) = S_3(0) = 1$, $T = 1$ year; weekly monitoring.

conditioning with respect to the systematic risk process, Z, and then integrating the Gram-Charlier A expansion of the density of the sum of the (exponential) idiosyncratic processes. In the special case of an equally-weighted homogeneous portfolio, computations can be simplified by convolving the density of the systematic process and the (log of the) Gram-Charlier A expansion.

4.2 Benchmarking and Testing

Numerical tests for the swap contract considered in this analysis are reported for the case of single trade in Table 2, in which we compare the unconditional survival probabilities obtained with both the FullMC approach and the hybrid MC+Hilbert method for $M_C = 10^5$ simulation trials. Moreover, we also report the uncollateralized CVA obtained using both methods. In the interest of a fair comparison, both methods employ the COS scheme for the computation of the option prices. We observe that the computational cost of the expected exposure is negligible; for example, the MC+Hilbert method with

$P = 2^9$ grid points estimates the CVA in 295 seconds, but the computation of the expected exposure takes only 9 seconds. The largest part of the CPU time is imputable, in fact, to the computation of survival probabilities. The hybrid MC+Hilbert algorithm exhibits a very good trade-off between accuracy and computational cost: Figure 2 shows that the curve of the CVA profile over time produced by our algorithm is very close to the one obtained by the FullMC(10^3) method; Table 2 shows though that the hybrid MC+Hilbert(2^9) approach is more than six times faster.

The quantification of the CVA becomes more computationally intensive in presence of the collateral agreements; our numerical tests show that, for $M_C \in \{10^5, 5 \times 10^5, 10^6\}$ the choice $\widehat{M} = 10^2$ for the bi-dimensional grid appears to provide the best trade-off between accuracy and computational cost. Indeed, this choice of $\widehat{M}$ does not affect the first six significant digits of the CVA, but it allows an important reduction of the computational cost. For example, for $M_C = 10^5$ simulation trials of the paths of the common factor Z, we have to evaluate the integrals at most $\widehat{M}^2$ times, instead of M_C times[5]; computational time: 1526 seconds instead of 21421 seconds for the case with unilateral agreement without MTA and initial margin.

Finally we consider the approximation of the CVA of a portfolio of swaps based on the Gram-Charlier A expansion. To test this approximation, we assume an equally-weighted homogeneous portfolio. These assumptions imply that (13) can be rewritten as

$$\Pi(t) = \alpha_3(t)\beta(t; a_3 Z))S_3(0)e^{(r-q_3-\varphi_{Y_3}(-i))t}\mathcal{Y}(t) - \bar{K}_3(t),$$

for $\mathcal{Y}$ as in (17). Therefore, the (conditional) independence of the terms in this summation suggests that, as alternative to the Gram-Charlier A expansion, the distribution of $\mathcal{Y}$ can be obtained by convolution through the characteristic function of Y_l, so that the basket option can be priced via numerical integration. However, as this characteristic function is in general not available in closed form, convolution needs to be performed numerically as well. The steps are as follows. Given the characteristic function of Y_l, which for Lévy processes is in general available in closed form, the inverse FFT is used to recover the density function of Y_l; the density function of e^{Y_l} follows by change of variable. Then, application of the direct FFT returns the characteristic function $\phi_{e^{Y_l}}(u;t)$ computed on a discrete grid $u_1, \cdots, u_P$ where P is the number of Fourier points. Consequently, the characteristic function of $\mathcal{Y}$ follows by (conditional) independence of the terms in the summation as $\phi_{\mathcal{Y}}(u;t) = \frac{1}{n-2}\prod_{l=3}^{n}\phi_{e^{Y_l}}(u;t)$, which is equal to $\frac{1}{n-2}\phi_{e^{Y_3}}(u;t)^{n-2}$ due to homogeneity. Finally, the density of $\mathcal{Y}$ is recovered using Fourier inversion once more.

The numerical tests show that the convolution procedure is very efficient if the number of assets in the portfolio is not too large (in our numerical experiments this happens if we have less than 20 assets), otherwise numerical errors accumulate and no reliable result is possible; on the other hand the Gram-Charlier A approximation works very well even for a small portfolio size. The left-hand panel of Figure 3 illustrates the expected exposure for an equally weighted and homogeneous portfolio of swap contracts in the uncollateralized case for $M_C = 10^5$, and portfolio size equal to 4, 7, 12. Even in the case of 4 assets, the distance in L^∞ norm between the expected exposure computed using

[5]As we exploit linear interpolation, we evaluate the integrals on the node $(Z^-_{j_1}, Z^+_{j_2})$, $j_1, j_2 = 0, \cdots \widehat{M} - 1$, if there exists m such that $(Z^{(m)}(t-\delta t), Z^{(m)}(t))$ belongs to the cell $(Z^-_{j_1-1}, Z^+_{j_2-1}) \times (Z^-_{j_1+1}, Z^+_{j_2+1}), m = 1, \cdots, M_C$.

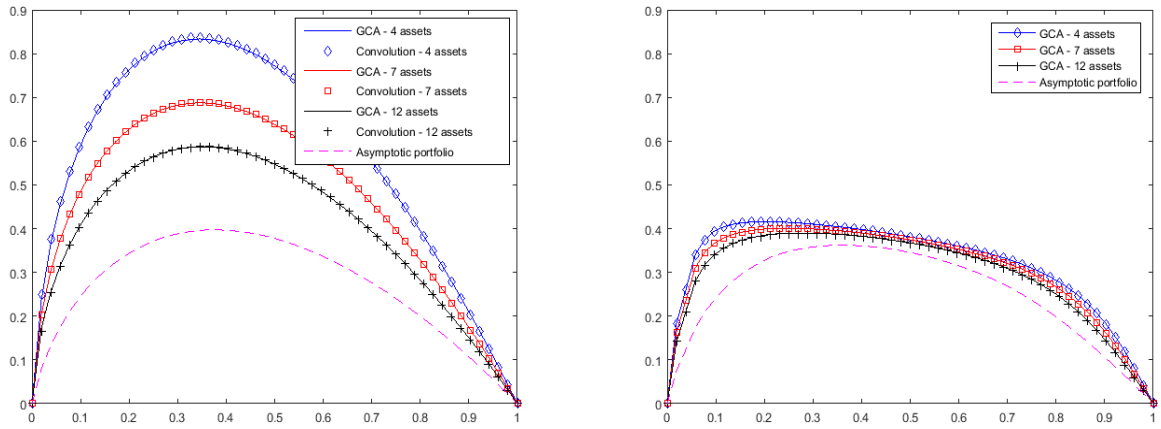

Figure 3: Netting: Convolution vs Gram-Charlier A Approximation. Uncollateralized (left) and Collateralized (right, unilateral collateral, $H_1 = 1$, $M = 0$) Expected Exposure computed for a basket of 4, 7, 12 homogeneous assets. Uncollateralized exposure: Corollary 6. Collateralized exposure: Proposition 2. Asymptotic portfolio: expected exposure in Corollary 7 (uncoll. exposure) and Corollary 3 (coll. exposure). Parameter set: Table 3. Other parameters: $S_1(0) = S_2(0) = S_3(0) = 1$, $T = 1$ year; weekly monitoring.

convolution and the Gram-Charlier A approximation is 0.01; this distance reduces to 0.003 (0.005) for 7 (12) assets. Moreover, the computational cost of the Gram-Charlier A approximation is half the one of the convolution method.

5 Case study: CVA of an oil commodity swap

In this Section, we use the developed framework to quantify the CVA originated by the swap contract analysed in Section 3.2, assuming that the relevant dynamics are given by the NIG process.

As mentioned in Section 1, we build a case study in the energy sector. Thus, for the specific example of our application, we initially consider a swap contract written on Brent Crude Oil. Further, we identify as counterparties in the swap a financial firm ('counterparty') and a corporate firm ('investor') in the energy sector. For illustrative purposes only, we have chosen Deutsche Bank (DB) as representative financial firm, and ENI as representative corporate firm.

In second instance, we explore the case of an equally weighted portfolio of swaps on homogeneous underlying assets.

All swap contracts are USD denominated and have 1 year tenor with weekly settlements corresponding to the difference between the index price at the closing of the week and the fixed swap price. For the case of Brent, the notional is 1 barrel of oil. The fixed swap price has been set to its no-arbitrage value and it has been computed according to the term structure of quoted index futures prices, linearly interpolating the missing maturities. DB is paying the fixed leg and receiving the floating leg.

5.1 Calibration

The most recent consultative paper Basel (2015a,b) and the subsequent response ISDA (2015b) recommend the calibration of internal models to be based on the joint use of credit spreads and equity data. Moreover, information on the default correlations should be based on either credit spreads or listed equity prices (see Laurent et al., 2016, as well). This is consistent with the dominant use of equity data among financial institutions to calibrate the default correlations. For this reason, we follow these recommendations and calibrate the model default probability to market credit spreads, whilst the default correlations are calibrated using historical equity market prices. The factor construction in (3) facilitates the calibration of the model in a relatively efficient way by means of a straightforward two steps calibration procedure.

In the first step, we obtain the parameters of the process chosen to model the margins $X_j(t)$, $j = 1, \ldots, n$, by direct calibration to market data. In the setting of Section 3, this is achieved by solving the following independent minimization problems

$$\min_{h_j, \lambda_j} \sum_{i=1}^{N} \left(CDS_j^{mkt}(0, T_i) - CDS^{model}(0, T_i; h_j, \lambda_j) \right)^2, \quad j = 1, 2, \tag{18}$$

$$\min_{\lambda_j} \sum_{i=1}^{M} \sum_{\iota=1}^{N} \left(O^{mkt}(K_i, T_\iota) - O^{model}(K_i, T_\iota; \lambda_j) \right)^2, \quad j = 3, \ldots, n. \tag{19}$$

In details. The minimization problem (18) is solved with respect to the unknown log-leverage $h_j = \ln(K_j/S_j(0))$ and the parameter set λ_j of the margin process X_j, $j = 1, 2$ (for example $\lambda_j \equiv (\theta_j, \sigma_j, k_j)$ in the case of the NIG process). Further, $CDS_j^{mkt}(0, T)$ denotes the market credit default spread for maturity T and counterparty j, whilst $CDS_j^{model}(0, T; h_j, \lambda_j)$ denotes the one computed according to the chosen model. The spread can be expressed in terms of marginal survival probability according to (see formula 6.5 page 107 in O'Kane, 2015)

$$CDS(0, T) = \frac{(1 - R)}{2} \frac{\sum_{k=1}^{N} \alpha_{k-1,k} \left(\mathbb{P}(\tau > t_{k-1}) - \mathbb{P}(\tau > t_k) \right) \left(P(0, t_{k-1}) + P(0, t_k) \right)}{\sum_{n=1}^{Np} \alpha_{n-1,n} \left(\mathbb{P}(\tau > t_{n-1}) + \mathbb{P}(\tau > t_n) \right) P(0, t_n)},$$

with $P(0, T)$ denoting the LIBOR discount curve[6] anchored to the credit default swap effective date, t_n, $n = 1, ..., Np$, the premium payment dates, t_k, $k = 1, ..., N$, the discrete default times and $\alpha_{i-1,i}$ the period tenors.

The minimization problems (19) - one per each position in the portfolio - are solved with respect to the parameter set of X_j, $j = 3, \ldots, n$; $O^{mkt}(K, T)$ is the market price of options on futures with strike K and time to maturity T, with the convention that we are using only out-of-the-money call and put options. Similarly, $O^{model}(K, T; \lambda_j)$ denotes the corresponding model price.

As mentioned in Section 4, the theoretical survival probability of the two counterparties is computed using the Hilbert transform as in (16) where f is now the density of the margin Lévy process X. The theoretical option prices are obtained using the COS method. As the quantities are therefore known in closed form (up to inversion), the procedure is fast and accurate. We randomize 100 times

[6] The relevant term structure of interest rates is bootstrapped using LIBOR and swap rates.

the initial parameter set around sensible starting values, and we select as starting value for the final calibration the average result obtained from the best 5 calibrations.

In the second step, we recover the parameters of the common factor and the idiosyncratic components given the parameter set of the margin processes obtained in the first step. The aim is to ensure that the loadings $\mathbf{a}$, and the parameter set λ_Z and λ_{Y_j} of the processes $Z(t)$ and $Y_j(t)$, $j = 1, \ldots, n$, respectively, are consistent and plausible with respect to the market quotations related to the margin processes. This procedure is subject to matching both the observed covariance matrix using the loading coefficients a_j, $j = 1, \ldots, n$, and the cumulants $K_s^{(\alpha)}$, $s = X, Y, Z$, of the margin processes by controlling for the parameters of the idiosyncratic components. Thus, we solve

$$\min_{\lambda_Z, \mathbf{a}, \lambda_\mathbf{Y}} \sum_{j=1}^{n} \int \left| \phi_{X_j}(u) - \phi_{Y_j}(u)\phi_Z(a_j u) \right|^2 du \tag{20}$$

$$\text{s.t} \quad \mathbb{C}ov^{market} - \mathbb{C}ov^{model}(\mathbf{a}) = 0 \tag{21}$$

$$K_{X_j}^{(\alpha)} - a_j^\alpha K_Z^{(\alpha)} - K_{Y_j}^{(\alpha)}(\lambda_{Y_j}) = 0 \quad \alpha = 1, ..., 4,\ j = 1, \ldots, n. \tag{22}$$

The objective function in (20) requires the match between the characteristic functions of the margin process and the one of the factor model (3). This choice is based on the extensive econometric literature on spectral estimation, where model parameters are estimated by fitting the theoretical characteristic function to the empirical one, see for example Feuerverger and Mureika (1977).

The constraint in (21) imposes the matching of the market and model covariance matrices. As proxy for the market covariance, $\mathbb{C}ov^{market}$, we use the sample historical covariance; the model covariance matrix for the adopted linear structure (3), instead, is $\mathbb{C}ov^{model}(\mathbf{a}) = \mathbf{a}\mathbf{a}'\mathbb{V}ar(Z(t))$. The use of the historical covariance is mainly due to the fact that in general products capable of providing information on the full covariance matrix are illiquid. The constraint in (22) ensures the matching between the cumulants of the idiosyncratic process implied by the factor model (3), once all other parameters are given. We bear in mind that fitting the cumulants amounts to fitting the characteristic function and its derivatives up to the maximum cumulant order considered but only at the origin. If the distribution to be recovered is fully determined by its moments, this is a plausible choice. A different motivation for using this procedure is given in Eriksson et al. (2009). We note that at single trade level, i.e. $n = 3$, with NIG dynamics, conditions (21)-(22) can be solved analytically with respect to ($\mathbf{a}$, $\lambda_\mathbf{Y}$), which reduces the optimization problem to an unconstrained minimization with respect to λ_Z only (see the Appendix for full details). However, the general optimization problem (20)-(22) applies regardless of the number of assets and/or the actual process used for modelling the relevant quantities.

For the single swap case, the calibrated parameters are reported in Table 3 together with the calibration performance as measured by the Root Mean Square Error (RMSE); we show the quality of the fitting in Figure 1 for the case of ENI; results relative to the other names are available upon request. We will use the same calibrated parameters at portfolio level under the assumption of homogeneous underlying assets, based on the fact that in this case the $n - 2$ idiosyncratic processes are independent copies.

a)	Margin Processes $X(t)$								
Name	K	q	θ	σ	k	Std. Dev	Skew	Exc. Kurt.	RMSE
DB	0.3324	0.0050	-0.2196	0.2460	0.5459	0.2947	-1.0972	2.4804	1.33E-03
ENI	0.5611	0.0136	-0.1846	0.0999	0.3361	0.1981	-0.8713	1.1435	1.29E-03
BRENT	-	0.0016	0.0683	0.1871	0.0796	0.1881	0.0866	0.2487	2.18E-03

b)	Idiosyncratic and systematic components							
	Correlation Matrix				Parameters			
	DB	ENI	BRENT	Process	β	γ	ν	a
DB	1.0000	-	-		-0.0917	0.1768	1.5826	0.3091
ENI	0.6468	1.0000	-	$Y(t)$	-0.0427	0.0157	1.5239	0.2040
BRENT	0.2151	0.2858	1.0000		0.1123	0.1761	0.0780	0.0871
				$Z(t)$	-0.7288	0.4719	0.4140	

Table 3: Calibrated parameters.Panel (a). Calibrated NIG model parameters. DB and ENI: calibrated to credit spreads. Brent Crude Oil: calibrated to option prices - settlement date: August 11, 2014; underlying futures quotation: 113.76 USD per barrel. Data Source: Markit, Chicago Mercantile Exchange. Observation date: June 26, 2014. Standard deviation, skewness and excess kurtosis (see Section 4) calculated using the reported parameters. RMSE: root mean squared error between market quotation and model price.
Panel (b). Correlation matrix and parameters of the idiosyncratic and systematics processes. Correlation matrix estimated using historical log-returns of DB, ENI and Brent Crude Oile (spot) over a 2 years period up to and including the observation date. Source: Yahoo! Finance and U.S. Energy Information Admin.
Components processes with characteristic exponent of the form $\varphi_{Y_j}(u) = (1 - \sqrt{1 - 2iu\beta_j\nu_j + u^2\gamma_j^2\nu_j})/\nu_j, j = 1, 2, 3$, $\varphi_Z(u) = (1 - \sqrt{1 - 2iu\beta_Z\nu_Z + u^2\gamma_Z^2\nu_Z})/\nu_Z$.

5.2 CVA, netting, Collateral and Wrong-Way Risk

In the following, we take the point of view of the corporate firm, so that the CVA is given by (6) in which the investor (Firm 2) is ENI and the counterparty (Firm 1) is DB. Particular emphasis is given to the sensitivity of the CVA to the level of correlation between the counterparty and the underlying asset, with the aim of analysing the effects of wrong-way risk. This can be defined as the impact on the CVA of positive dependence between the counterparty probability of default and the marked to market value of the position. In our framework, this occurs when $\rho_{13} < 0$. If, instead, $\rho_{13} > 0$, we observe effects of right-way risk. The analysis is carried out by perturbing ρ_{13} about its estimated value, re-fitting the model parameters according to the new correlation matrices following the procedure given in Section 5.1, and re-computing the CVA.

In Figure 4, we report the profiles of the uncollateralized CVA (in absence of IM) for a single swap contract obtained in correspondence of different values of the correlation coefficient ρ_{13}. The right-hand side panel shows the effect of positive correlation: the higher ρ_{13}, the lower the corresponding CVA. Higher positive correlation, in fact, implies a higher probability that the exposure moves out-of-the-money as the credit quality of counterparty deteriorates, reducing the counterparty credit risk for the investor (right-way risk effect). The left-hand side panel instead shows the wrong-way risk effect as the CVA increases the more 'anti-correlated' the counterparty and the underlying assets are.

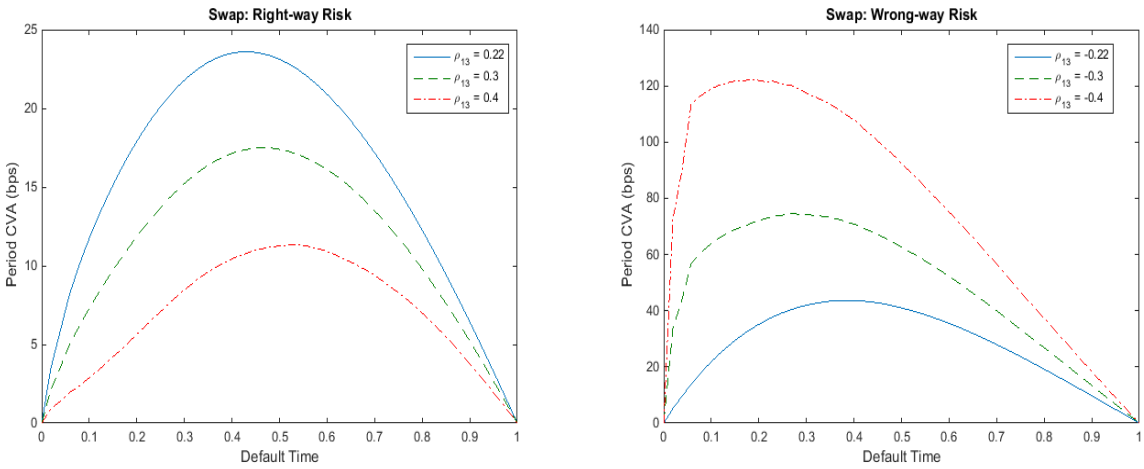

Figure 4: Uncollateralized CVA - Right-way Risk and Wrong-way Risk. Swap contract. Parameter set: Table 3. Other parameters: $S_1(0) = S_2(0) = S_3(0) = 1$, $T = 1$ year. Weekly monitoring. MC+Hilbert: 10^6 simulation trials, 2^{10} grid points. COS: 2^9 grid points, $L = 15$.

The more negative ρ_{13} is, in fact, the higher the probability of an adverse movement in both the exposure and the credit quality of the counterparty. We note the shape of the CVA profile which is originated by the payment schedule of the product under consideration. The swap contract, in fact, is a multiple cash-flow product; consequently after an initial period in which the exposure increases, i.e. the so-called diffusion effect is predominant, the exposure decreases as the amount left to settle decreases ('amortization' effect). Similar considerations hold for other contracts, although the shape of the CVA profile would change according to the contracts payment schedule (see the Appendix for an example based on a forward contract).

The total CVA faced by Firm 2 corresponding to the profiles of the swap contract shown in Figure 4 is reported in panel (a) of Table 4, together with the corresponding 95% confidence interval. We notice that for the case under consideration, the uncollateralized CVA can be reduced by up to 55% due to right-way risk, whilst it can increase by more than 4 times due to wrong-way risk.

In Table 4 - panel (a) we also report the impact of the bilateral agreement for collateralization on the CVA, computed as the (percentage) difference between the collateralized CVA and the corresponding uncollateralized one, together with the impact of the Initial Margin (computed in a similar way). In this analysis we set the triggering thresholds H_1, H_2 to their tighest possible level, and we ignore mitigation effects due to MTA. This specification corresponds to the latest Uncleared Margin Rules for bilateral trading (see, for example, Andersen et al., 2017, and references therein). For a fuller analysis of the impact of the thresholds, we refer the interested reader to Appendix E.

We notice that in all cases, the CVA reduces compared to the uncollateralized case; the collateral agreements are particularly effective in presence of right-way risk. Wrong-way risk on the other hand reduces the effectiveness of the collateralization as, when $\rho_{13} < 0$, increases in the value of S_3 are more likely to be associated with a worsening of the counterparty probability of default, which counteracts the mitigation effect offered by the collateral posting in the investor's favour. For what concerns the impact of the initial margin on both uncollateralized and collateralized CVA, we observe the very strong 'smoothing' effect of the initial margin on CVA regardless of the correlation scenario and the

a) Single Trade	Right-way Risk			Wrong-way Risk		
scenario: s	1	2	3	4	5	6
Uncoll. CVA (bps)	820.2608	600.4706	368.9231	1458.0926	2590.5305	4119.8749
95% C.I.	819.8556	599.8578	368.0877	1455.6966	2581.9565	4105.7774
	820.6660	601.0834	369.7585	1460.4887	2599.1046	4133.9723
Collateral agreement impact	-78.05%	-77.13%	-76.75%	-66.76%	-44.89%	-31.84%
Initial Margin impact without Collateral	-77.64%	-78.2%	-80.89%	-71.14%	-64.61%	-57.64%
Initial Margin impact with Collateral	-98.41%	-97.94%	-97.08%	-97.24%	-88.72%	-79.64%
b) Portfolio of Trades (25 homogeneous assets)						
s	1	2	3	4	5	6
Uncoll. CVA (bps)	176.3765	98.7591	27.6611	817.8735	2094.3232	3847.7627
95% C. I.	176.2083	98.6604	27.6263	814.6361	2081.3423	3826.1269
	176.5448	98.8577	27.6960	821.1108	2107.3042	3869.3985
Collateral agreement impact	-62.32%	-52.40%	-21.63%	-53.44%	-34.85%	-27.35%
Initial Margin impact without Collateral	-94.36%	-95.88%	-97.06%	-38.90%	-26.30%	-21.97%
Initial Margin impact with Collateral	-99.50%	-98.85%	-96.08%	-75.02%	-53.84%	-45.44%

Table 4: CVA, Righ/Wrong-Way Risk, Collateral & Initial Margin. Right-Way Risk Scenarios - $s = 1$: $\rho_{13} = 0.2151$ (benchmark); $s = 2$: $\rho_{13} = 0.3$; $s = 3$: $\rho_{13} = 0.4$. Wrong-Way Risk Scenarios - $s = 4$: $\rho_{13} = -0.2151$ (benchmark); $s = 5$: $\rho_{13} = -0.3$; $s = 6$: $\rho_{13} = -0.4$. Other correlations: Table 3. Other parameters: $S_1(0) = S_2(0) = S_3(0) = 1$, $T = 1$ year. Weekly monitoring. Impact of collateral and IM agreements computed as $(Coll.CVA_s - Uncoll.CVA_s)/Uncoll.CVA_s$ or $((Coll.+IM)CVA_s - Uncoll.CVA_s)/Uncoll.CVA_s$. Thresholds: $H_1 = H_2 = M = 0$. MC+Hilbert: 10^6 simulation trials, 2^9 grid points. COS: 2^9 grid points, $L = 15$.

collateral scheme in place. Indeed the initial margin manages to mitigate a large percentage of the residual risk generated by situations of strong wrong-way risk. In this respect, the initial margin and collateral play a complementary role in the reduction of the CVA, with the initial margin becoming the main player especially in presence of wrong-way risk. Consequently, the initial margin is fundamental in controlling gap risk.

This form of residual risk is illustrated in Figure 5, in which we report the probability of a gap event given in (12) for different levels of possible variations in the underlying variables. As in presence of initial margin the percentage variation in the stock necessary to trigger the gap event has to be quite consistent, Figure 5 highlights that the higher the initial margin, the lower the probability of the gap event. Figure 5 also confirms the need of a distribution with slowly decaying tails for an accurate quantification of this risk in a structural framework. Although the NIG process chosen for this experiment satisfies this property, models based on the Gaussian distribution would return a (almost) zero probability of gap risk even in presence of significant wrong-way risk (we note the different y-axis scale between the plot on the left-hand side of Figure 5 and the one on the right-hand side).

We turn now our attention to the portfolio case, under the assumption of equal weights and homogeneous underlyings, as in Section 4.2. Under these simplifying assumptions, the case in which netting agreements are not permitted coincides with the single trade one considered above (without collateral clauses). Results are reported in Table 4 - panel (b), in which we consider an illustrative case with 25 assets. The impact of different portfolio sizes is illustrated - for the benchmark scenario - in Figure 3, in which we observe that the risk mitigation with respect to the situation of no netting

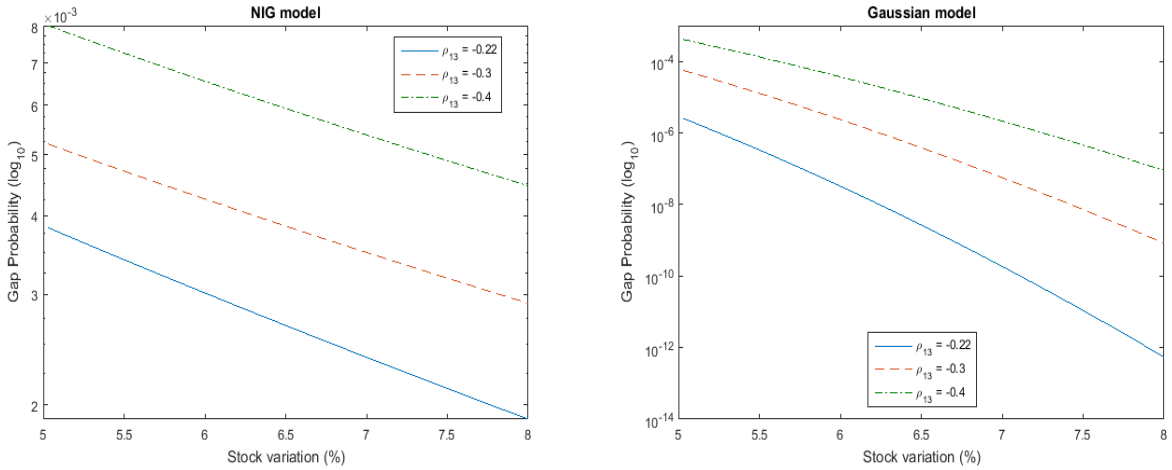

Figure 5: Gap Risk - Swap Contract. Gap Probability: Proposition 4. Two weeks lag. Wrong-Way Risk scenarios. NIG Margin Parameters: Table 3. Gaussian Margin Parameters: $\sigma_1 = 13.95\%$, $\sigma_2 = 14.25\%$, $\sigma_3 = 18.03\%$.

is significant already for as few as 4 contracts, and it improves by further increasing the size of the portfolio. By comparing the two panels of Figure 3 we notice the significant reduction in the portfolio CVA due to collateralization, to the extent that the impact of netting is now significantly reduced, and the marginal benefit of adding contracts in the portfolio is diminishing. In Figure 3 we also show the case of the asymptotic portfolio, as from Corollary 3. Panel (b) in Table 4, though, shows that the netting mitigation is significantly affected in presence of strong wrong-way risk. We also notice the relatively reduced effectiveness of collateralization, due to the already in place compensation provided by the aggregation of trades. The initial margin, on the other hand, still proves to be a strong risk mitigation tool.

The choice of the underlying assets of the contracts included in the portfolio is important as to maximize the effect of netting clauses, as shown in Figure 6. In the cases of both 'crude' CVA and collateralized CVA (without initial margin) reported in the left-hand and centre panels of Figure 6, netting is more effective the more decorrelated the assets, whilst in presence of high levels of linear correlation, there is almost no mitigation effect on the exposure offered by increasing the portfolio size. However, the initial margin can provide support to the aggregation of trades: the right-hand panel of Figure 6 shows in fact that in presence of initial margin, even without collateral, the expected exposure becomes almost insensitive to the level of diversification as the portfolio size increases. Hence, the initial margin provides mitigation even towards residual risk due to low diversification. One final consideration though is in order. As the initial margin depends on the portfolio composition, it is affected as well by the smoothing action of the netting mechanism. This explains why the asymptotic portfolio is no longer able to offer the maximum possible reduction in presence of low levels of diversification. Hence, the right-hand panel of Figure 6 shows that, in presence of high levels of linear correlation between the underlying assets, netting might not be the most convenient tool for risk mitigation.

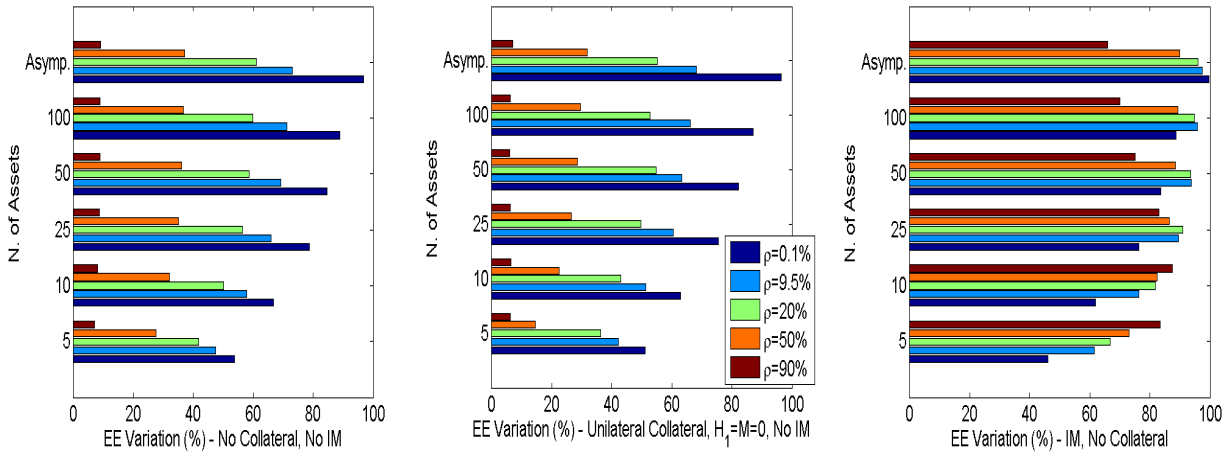

Figure 6: Netting: Swap on a basket of homogeneous assets. Diversification induced by varying correlation amongst assets in the portfolio for the uncollateralized case (left), unilateral collateral case ($H_1 = M = 0$, center), both without IM, and the uncollateralized case with IM (right). Parameter set: Table 3. Other parameters: $S_1(0) = S_2(0) = S_3(0) = 1$, $T = 1$ year, $H_1 = 1$, $M = 0$. Weekly monitoring. MC+Hilbert: $M_C = 10^6$ simulation trials, 2^9 grid points.

6 Conclusion

We proposed a general framework for the quantification of CVA in the setting of a structural model based on multivariate Lévy processes, with wrong/right-way risk captured endogenously. By means of fast and accurate numerical strategies for model calibration and CVA computation in presence of several mitigating clauses such as collateral, initial margin and netting, we have shown that the proposed approach can deal with the complex CVA design. We used this setting to gain insights into the delicate interactions between several aspects of the CVA calculation.

Nevertheless, the proposed approach shares with the other ones mentioned in the literature a few shortcomings. One of these is due t market incompleteness. Hedging CVA is per se a non trivial task also due to the inherent incompleteness of credit markets. The degree of incompleteness is though exacerbated by assumption of purely discontinuous driving processes. A more general shortcoming is related to the information quality on input and data: often the implementation of CVA valuation models faces obstacles generated for example by lack of a liquid credit curve for the counterparties, and uncertainty in recovery rates (see Brigo et al., 2013b, for example). However, these difficulties are intrinsic in the general counterparty risk valuation and management issue.

A promising route for further research could be the pairing of our approach with the wrong way set of equivalent measures developed by Brigo and Vrins (2018) for (unilateral) CVA in an intensity setting. Brigo and Vrins (2018) approach allows to 'remove' dependence - so to speak - so that the Monte Carlo simulation stage of the CVA computation can be bypassed. Thus, it would be very interesting to study the possible extension of this change of measure approach to bilateral CVA in the context of the structural model, in order to tackle the open issue of lack of analytical tractability of CVA in presence of dependence, and improve its practical use.

Acknowledgments

The Authors would like to thank Stéphane Crépey, Ernst Eberlein, Geneviéve Gauthier, Emmanuel Gobet, Massimo Morini, Andrea Pallavicini, Wolfgang Runggaldier for useful comments and suggestions. This paper has been presented at the 2nd International Conference on Computational Finance, ICCF 2017, the 3rd Symposium on Quantitative Finance and Risk Analysis, QFRA 2017, the Energy and Commodity Finance Conference 2016, the EURO Working Group for Commodities and Finance Modelling 2016, the Eighth World Congress of the Bachelier Finance Society, the conference 'Challenges in Derivatives Markets: Fixed income modeling, valuation adjustments, risk management, and regulation', the 2015 EMLYON Quant 12 Workshop, the 2015 AMASES Conference, the 2015 London-Paris Bachelier Mathematical Finance Workshop, the 2014 Summer School on Risk Management in Rome, and seminars at Université catholique de Louvain, Université libre de Bruxelles, Imperial College London, Prometeia in Bologna, Banca IMI in Milan, and the Nomura Centre for Mathematical Finance in Oxford. We thank all the participants for their helpful feedback. Usual caveat applies.

References

Andersen, L.B.G., Pykhtin, M., Sokol, A., 2017. Credit exposure in the presence of initial margin. Available at SSRN.

Ayadi, M.A., Ben-Ameur, H., Fakhfakh, T., 2016. A dynamic program for valuing corporate securities. European Journal of Operational Research 249, 751–770.

Ballotta, L., Bonfiglioli, E., 2016. Multivariate asset models using Lévy processes and applications. The European Journal of Finance 22, 1320–1350.

Ballotta, L., Deelstra, G., Rayée, G., 2017. Multivariate FX models with jumps: triangles, quantos and implied correlation. European Journal of Operational Research 260, 1181–1199.

Ballotta, L., Fusai, G., 2015. Counterparty credit risk in a multivariate structural model with jumps. Finance, Revue de l'Association Française de Finance 36, 39–74.

Barndorff-Nielsen, O., Pedersen, B.V., 1979. The Bivariate Hermite Polynomials up to Order Six. Scandinavian Journal of Statistics 6, 127–128.

Barndorff-Nielsen, O.E., 1995. Normal inverse Gaussian distributions and the modeling of stock returns. Research report 300. Department of Theoretical Statistics, Aarhus University.

Basel, 2010. Basel III: A global regulatory framework for more resilient banks and banking systems.

Basel, 2013. Regulatory Consistency Assessment Programme (RCAP) - Second report on risk-weighted assets for market risk in the trading book.

Basel, 2015a. Fundamental review of the trading book: Outstanding issues (consultative paper 3).

Basel, 2015b. Instructions for Basel III: monitoring - version for banks providing data for the trading book part of the exercise.

Bielecki, T., Brigo, D., Patras, F., 2011. Credit Risk Frontiers: Subprime Crisis, Pricing and Hedging, CVA, MBS, Ratings, and Liquidity. Wiley Finance/Bloomberg Book.

BIS, 2011. Basel Committee finalises capital treatment for Bilateral Counterparty Credit Risk.

Black, F., Cox, J., 1976. Valuing corporate securities: some effects of bond indenture provisions. Journal of Finance 31, 351–367.

Brigo, B., Buescu, C., Morini, M., 2012. Counterparty risk pricing: impact of closeout and first-to-default times. International Journal of Theoretical and Applied Finance 15.

Brigo, D., Bakkar, I., 2009. Accurate counterparty risk valuation for energy-commodities swaps. Energy Risk 6, 106–111.

Brigo, D., Capponi, A., Pallavicini, A., 2014. Arbitrage-free bilateral counterparty risk valuation under collateralization and application to credit default swaps. Mathematical Finance 24, 125–146.

Brigo, D., Capponi, A., Pallavicini, A., Papatheodorou, V., 2013a. Pricing counterparty risk including collateralization, netting rules, re-hypothecation and wrong-way risk. International Journal of Theoretical and Applied Finance 16, 1350007.

Brigo, D., Masetti, M., 2006. Risk neutral pricing of counterparty risk, in: Pykhtin, M. (Ed.), Counterparty Credit Risk Modelling: Risk Management. Risk Books London. chapter 11.

Brigo, D., Morini, M., Pallavicini, A., 2013b. Counterparty Credit Risk, Collateral and Funding. Wiley John & Sons.

Brigo, D., Morini, M., Tarenghi, M., 2011. Credit calibration with structural models and equity return swap valuation under counterparty risk, in: Bielecki, T, R., Brigo, D., Patras, F. (Eds.), Credit Risk Frontiers: Subprime Crisis, Pricing and Hedging, CVA, MBS, Ratings, and Liquidity. Bloomberg Financial Series. chapter 14, pp. 457–484.

Brigo, D., Vrins, F., 2018. Disentangling wrong-way risk: pricing credit valuation adjustment via change of measures. European Journal of Operational Research .

Chen, N., Kou, S.G., 2009. Credit spreads, optimal capital structure, and implied volatility with endogenous default and jump risk. Mathematical Finance 19, 343–378.

Cont, R., Tankov, P., 2004. Financial modelling with Jump Processes. Chapman & Hall/CRC Press.

Crépey, S., Bielecki, T.R., Brigo, D., 2014. Counterparty risk and funding: A tale of two puzzles. CRC Press.

Davidson, C., 2008. Speed tests. Risk 21, 59–61.

Embrechts, P., McNeil, A., Straumann, D., 2002. Correlation and dependence in risk management: properties and pitfalls, in: Dempster, M. (Ed.), Risk management: Value at risk and beyond. Cambridge University Press, pp. 176–223.

Eriksson, A., Ghysels, E., Wang, F., 2009. The Normal Inverse Gaussian distribution and the pricing of derivatives. The Journal of Derivatives 16, 23–37.

Fang, F., Oosterlee, C.W., 2008. A novel pricing method for European options based on Fourier-Cosine series expansions. SIAM Journal on Scientific Computing 31, 826–848.

Feng, L., Linetsky, V., 2008. Pricing discretely monitored barrier options and defaultable bonds in Lévy process models: A fast Hilbert transform approach. Mathematical Finance 18, 337–384.

Feuerverger, A., Mureika, R.A., 1977. The empirical characteristic function and its applications. Ann. Statist. 5, 88–97.

Gregory, J., 2015. The xVA Challenge: Counterparty Credit Risk, Funding, Collateral, and Capital. Wiley. third edition.

ISDA, 2010. The importance of close-out netting.

ISDA, 2014. ISDA Margin Survey 2014.

ISDA, 2015a. ISDA Margin Survey 2015.

ISDA, 2015b. Letters on the fundamental review of the trading book.

Itkin, A., Lipton, A., 2015. Efficient solution of structural default models with correlated jumps and mutual obligations. International Journal of Computer Mathematics 92, 2380–2405.

Kim, J., Leung, T., 2016. Pricing derivatives with counterparty risk and collateralization: A fixed point approach. European Journal of Operational Research 249, 525 – 539.

Laurent, J., Sestier, M., Thomas, S., 2016. Trading book and credit risk: How fundamental is the Basel review? Journal of Banking & Finance 73, 211 – 223.

Mardia, K.V., 1970. Families of Bivariate Distributions. Griffin's Statistical Monographs, Lubrecht & Cramer Ltd.

McNeil, A.J., Rüdiger, F., Embrechts, P., 2015. Quantitative Risk Management. University Press Group Ltd.

Noonan, L., McLannahan, B., 2015. US banks hit by cheap oil as Opec warns of long-term low. Financial Times. December 24th .

Oh, D.H., Patton, A.J., 2017. Modelling dependence in high dimensions with factor copulas. Journal of Business & Economic Statistics 35, 139–154.

O'Kane, D., 2015. Modelling Single-name and Multi-name Credit Derivatives. Wiley John & Sons.

Polley, M., 2016. Die Edgeworth-Approximation zur Kalibrierung eines Lévy-Hybridmodells unter dem physikalischen Maß. Ph.D. thesis. Fakultät für Mathematik und Physik der Albert-Ludwigs-Universität Freiburg im Breisgau.

Pykhtin, M., 2011. Counterparty Risk Management and Valuation, in: Bielecki, T, R., Brigo, D., Patras, F. (Eds.), Credit Risk Frontiers: Subprime Crisis, Pricing and Hedging, CVA, MBS, Ratings, and Liquidity. Bloomberg Financial Series. chapter 16, pp. 507–536.

Rodrigues, V., Crooks, E., 2015. Default risk in US oil and gas sector. Financial Times. February 2nd .

Stuart, A., Ord, K., 1994. Kendall's Advanced Theory of Statistics, Distribution Theory. volume 1. Wiley.

Vašíček, O., 1987. Probability of loss on loan portfolio. Memo. San Francisco: KMV Corporation.

Wu, L., 2015. CVA and FVA to derivatives trades collateralized by cash. International Journal of Theoretical and Applied Finance 18.

A Proof of Propositions

A.1 Proof of Proposition 1

For the case of the swap contract with value function (11), we note that

$$v(t,S_3)=\alpha_3(t)\beta(t;a_3Z)S_3(0)e^{(r-q_3-\varphi_{Y_3}(-i))(t-\delta t)+Y_3(t-\delta t)}e^{(r-q_3-\varphi_{Y_3}(-i))\delta t+Y_3'(\delta t)}-\bar{K}_3(t),$$

where Y_3' is an independent copy of Y_3. By the same argument

$$\begin{aligned}\Pi^p(\Pi(t-\delta t),\Delta t) &= \alpha_3(t-\delta t+\Delta t)\beta(t-\delta t;a_3Z)S_3(0)e^{(r-q_3-\varphi_{Y_3}(-i))(t-\delta t)+Y_3(t-\delta t)}e^{(r-q_3-\varphi_{X_3}(-i))\Delta t+X_3^p(\Delta t)}\\ &\quad -\bar{K}_3(t-\delta t+\Delta t).\end{aligned}$$

Due to independence of the increments, the result then follows by conditioning on the value of the idiosyncratic process Y_3 at time $t-\delta t$, and considering $X_3^p(\Delta t)$ as fixed.

A.2 Proof of Proposition 2

As stated in Section 3.4, the bivariate process $(\Pi(t),\Pi(t-\delta t))$ is described by the mean vector (m_1,m_2) and the covariance matrix $(\sigma_1^2,\sigma_{12};\sigma_{12},\sigma_2^2)$. Simple computations lead to

$$m_1=\mathbb{E}_Z(\Pi(t))=\sum_{l=3}^{n+2}w_l\left(\alpha_l(t)\beta(t;a_3Z)S_l(0)\,e^{\left(r-q-\phi_{Y_l}(-i)\right)t}\mathbb{E}\left(e^{Y_l(t)}\right)-\bar{K}_l(t)\right),$$

$$m_2=\mathbb{E}_Z(\Pi(t-\delta t))=\sum_{l=3}^{n+2}w_l\left(\alpha_l(t-\delta t)\beta(t-\delta t;a_3Z)S_l(0)\,e^{\left(r-q-\phi_{Y_l}(-i)\right)(t-\delta t)}\mathbb{E}\left(e^{Y_l(t-\delta t)}\right)-\bar{K}_l(t)\right),$$

$$\sigma_1^2=\mathbb{V}ar_Z(\Pi(t))=\sum_{l=3}^{n+2}w_l^2\alpha_l^2(t)\beta^2(t;a_3Z)S_l^2(0)\,e^{2\left(r-q-\phi_{Y_l}(-i)\right)t}\left(\mathbb{E}\left(e^{2Y_l(t)}\right)-\mathbb{E}^2\left(e^{Y_l(t)}\right)\right),$$

$$\sigma_2^2=\mathbb{V}ar_Z(\Pi(t-\delta t))=\sum_{l=3}^{n+2}w_l^2\alpha_l^2(t-\delta t)\beta^2(t-\delta t;a_3Z)S_l^2(0)\,e^{2\left(r-q-\phi_{Y_l}(-i)\right)(t-\delta t)}\left(\mathbb{E}\left(e^{2Y_l(t-\delta t)}\right)-\mathbb{E}^2\left(e^{Y_l(t-\delta t)}\right)\right),$$

$$\begin{aligned}\sigma_{12}=\mathbb{C}ov_Z(\Pi(t-\delta t),\Pi(t))&=\sum_{l=3}^{n+2}w_l^2\alpha_l(t-\delta t)\beta(t-\delta t;a_3Z)\alpha_l(t)\beta(t;a_3Z)S_l^2(0)\,e^{\left(r-q-\phi_{Y_l}(-i)\right)(t-\delta t)+\left(r-q-\phi_{Y_l}(-i)\right)(t)}\\ &\quad\times\left(\mathbb{E}\left(e^{Y_l(t)-Y_l(t-\delta t)}\right)\mathbb{E}\left(e^{2Y_l(t-\delta t)}\right)-\mathbb{E}\left(e^{Y_l(t)}\right)\mathbb{E}\left(e^{Y_l(t-\delta t)}\right)\right).\end{aligned}$$

The expected values in the above summations can be easily recovered from the characteristic function of Y_l. The same applies to the co-cumulant $K_{\mathbf{\Pi}}^{\boldsymbol{\alpha}}$ once these are expressed in term of the raw co-moments, as in Stuart and Ord (1994). Consider now the standardized processes $\xi_1=(\Pi(t)-m_1)/\sigma_1,\xi_2=(\Pi(t-\delta t)-m_2)/\sigma_2$; the generic payoff (7) can then be rewritten as

$$(\alpha\xi_1+\beta\xi_2+\gamma)^+\,1_{(\varepsilon_l<\xi_2<\varepsilon_u)}$$

for

$$\alpha=A\sigma_1;\beta=-(B+D)\sigma_2;\gamma=Am_1-(B+D)m_2+C+D\Pi^p(\xi_2\sigma_2+m_2,\Delta t);\varepsilon_l=\frac{E-Dm_2}{D\sigma_2};\varepsilon_u=\frac{F-Dm_2}{D\sigma_2}.$$

Given the nature of the 2-dimensional Hermite polynomials and the decomposition of the bivariate standard normal density function, the expected value of the above payoff can be written as

$$\int_{\mathbb{R}} 1_{(\varepsilon_l<\xi_2<\varepsilon_u)} \frac{e^{-\frac{\xi_2^2}{2}}}{\sqrt{2\pi}} \int_{\mathbb{R}} (\alpha\xi_1+\beta\xi_2+\gamma)^+ \frac{e^{-\frac{(\xi_1-\rho\xi_2)^2}{2(1-\rho^2)}}}{\sqrt{2\pi(1-\rho^2)}} \left(1+\sum_{|\boldsymbol{\alpha}|=3}^{4} \frac{K_{\boldsymbol{\xi}}^{\boldsymbol{\alpha}}}{\boldsymbol{\alpha}!} \sum_{i,j=0}^{|\boldsymbol{\alpha}|} h_{i,j}^{\boldsymbol{\alpha}} \xi_1^i \xi_2^j\right) d\xi_1 d\xi_2.$$

The required result follows from the truncated moments of the normal distribution and by noting that the (conditional) mean and variance of ξ_1, i.e. $\rho\xi_2$ and $1-\rho^2$, once re-expressed for the non-standardized quantity, return

$$m_1 + \frac{\sigma_{12}}{\sigma_2^2}(y-m_2) =: m_{1|2}(y),$$
$$\sigma_1^2 - \frac{\sigma_{12}^2}{\sigma_2^2} =: \sigma_{1|2}^2.$$

The expression of the coefficients $h^{\boldsymbol{\alpha}}$ can be recovered from the explicit expressions in Barndorff-Nielsen and Pedersen (1979); for example for the case $\boldsymbol{\alpha}=(3,0)$, the relevant coefficients are $h_{0,1}^{(3,0)} = -3\zeta_{11}\zeta_{12}$, $h_{0,3}^{(3,0)} = \zeta_{12}^3$, $h_{1,0}^{(3,0)} = -3\zeta_{11}^2$, $h_{1,2}^{(3,0)} = 3\zeta_{11}\zeta_{12}^2$, $h_{2,1}^{(3,0)} = 3\zeta_{11}^2\zeta_{12}$, $h_{3,0}^{(3,0)} = \zeta_{11}^3$, whilst all remaining terms are zero, and ζ_{ij} is the element in position ij of the matrix Σ^{-1}. The coefficients of all other Hermite polynomials can be derived following the same procedure.

B Gap Risk

Let us assume that the t-value function of the contract is of the form (11), the following result holds.

Proposition 4 *Consider the multivariate structural model described by equations (2)-(3) and the probability of a gap event as defined in (12). Then $P_{Gap}>0$ if and only if $\rho_{13}<0$ for all $t>0$. Further, set $\varepsilon_j = (r-q_j-\varphi_j(-i))\delta t + \Delta_j$, $j=1,2$ and $\varepsilon_3 = \varphi_3(-i)\delta t + \Delta_3$, with $\Delta_j>0$, $j=1,2,3$. Then, for $\Delta_j \uparrow \infty$, $j=1,2,3$,*

$$P_{Gap} = \begin{cases} \mathbb{P}\left(\max\left\{\frac{\varepsilon_1}{|a_1|}, \frac{\varepsilon_3}{a_3}\right\} < Z(t)-Z(t-\delta t) < \frac{\varepsilon_2}{|a_2|}\right) & a_1,a_2<0<a_3 \\ \mathbb{P}\left(-\frac{\varepsilon_2}{a_2} < Z(t)-Z(t-\delta t) < \min\left\{-\frac{\varepsilon_1}{a_1}, -\frac{\varepsilon_3}{|a_3|}\right\}\right) & a_3<0<a_1,a_2 \\ \mathbb{P}\left(Z(t)-Z(t-\delta t) > \max\left\{\frac{\varepsilon_1}{|a_1|}, \frac{\varepsilon_3}{a_3}\right\}\right) & a_1<0<a_2,a_3 \\ \mathbb{P}\left(Z(t)-Z(t-\delta t) < \min\left\{-\frac{\varepsilon_1}{a_1}, -\frac{\varepsilon_3}{|a_3|}\right\}\right) & a_2,a_3<0<a_1, \end{cases}$$

which is well defined if

$$\begin{cases} \varepsilon_2 > |a_2| \max\left\{\frac{\varepsilon_1}{|a_1|}, \frac{\varepsilon_3}{a_3}\right\} & a_1,a_2<0<a_3 \\ \varepsilon_2 > -a_2 \min\left\{-\frac{\varepsilon_1}{a_1}, -\frac{\varepsilon_3}{|a_3|}\right\} & a_3<0<a_1,a_2. \end{cases}$$

This result is a generalization of Ballotta et al. (2017) and the proof follows the same steps. The main observation is that the probability of sums of random variables all exceeding some diverging threshold is driven completely by the common component of the sums (see Oh and Patton, 2017, for example). Thus, we note that for $v(t)$ of the form in (11),

$$\begin{aligned} P_{Gap} &= \mathbb{P}\left(X_1(t)<l_1(t), X_2(t)\geq l_2(t), X_3(t)>l_3(t) \middle| X_1(t-\delta t)=l_1(t-\delta t)+\Delta_1,\right. \\ &\qquad \left. X_2(t-\delta t)=l_2(t-\delta t)+\Delta_2, X_3(t-\delta t)=l_3(t-\delta t)-\Delta_3\right) \end{aligned}$$

with $l_j(t)=h_j-\hat{\mu}_j t$ for $j=1,2$, and $l_3(t)=\ln\left(\bar{K}_3(t)/(\alpha(t)S_3(0))\right)-\hat{\mu}_3 t$. Denote $\delta X_j(t)=X_j(t)-X_j(t-\delta t)$ for $j=1,2,3$, the increment of the process X_j over the relevant period of time. By property of independent

and stationary increments of the Lévy process $X_j(t)$, it follows that

$$\begin{aligned} P_{Gap} &= \mathbb{P}\left(\delta X_1(t) < -\varepsilon_1, \delta X_2(t) \geq -\varepsilon_2, \delta X_3(t) > \varepsilon_3\right) \\ &\approxeq \mathbb{P}\left(-a_1\delta Z(t) > \varepsilon_1, a_2\delta Z(t) > -\varepsilon_2, a_3\delta Z(t) > \varepsilon_3\right). \end{aligned} \tag{B.1}$$

If $\rho_{13} > 0$ for all $t > 0$, we obtain from (B.1)

$$P_{Gap} = \begin{cases} \mathbb{P}\left(\delta Z(t) < -\frac{\varepsilon_1}{a_1}, \delta Z(t) > -\frac{\varepsilon_2}{a_2}, \delta Z(t) > \frac{\varepsilon_3}{a_3}\right) & a_1, a_2, a_3 > 0 \\ \mathbb{P}\left(\delta Z(t) > \frac{\varepsilon_1}{|a_1|}, \delta Z(t) < \frac{\varepsilon_2}{|a_2|}, \delta Z(t) < -\frac{\varepsilon_3}{|a_3|}\right) & a_1, a_2, a_3 < 0 \\ \mathbb{P}\left(\delta Z(t) < -\frac{\varepsilon_1}{a_1}, \delta Z(t) < \frac{\varepsilon_2}{|a_2|}, \delta Z(t) > \frac{\varepsilon_3}{a_3}\right) & a_2 < 0 < a_1, a_3 \\ \mathbb{P}\left(\delta Z(t) > \frac{\varepsilon_1}{|a_1|}, \delta Z(t) > -\frac{\varepsilon_2}{a_2}, \delta Z(t) < -\frac{\varepsilon_3}{|a_3|}\right) & a_1, a_3 < 0 < a_2. \end{cases}$$

Therefore P_{Gap} is zero. On the other hand, if $\rho_{13} < 0$ for all $t > 0$, we distinguish between the following cases.

a) $a_1, a_2 < 0 < a_3$; then (B.1) returns

$$\begin{aligned} P_{Gap} &= \mathbb{P}\left(\delta Z(t) > \frac{\varepsilon_1}{|a_1|}, \delta Z(t) < \frac{\varepsilon_2}{|a_2|}, \delta Z(t) > \frac{\varepsilon_3}{a_3}\right) \\ &= \mathbb{P}\left(\max\left\{\frac{\varepsilon_1}{|a_1|}, \frac{\varepsilon_3}{a_3}\right\} < \Delta Z(t) < \frac{\varepsilon_2}{|a_2|}\right), \end{aligned}$$

which is non-zero if

$$\varepsilon_2 > |a_2| \max\left\{\frac{\varepsilon_1}{|a_1|}, \frac{\varepsilon_3}{a_3}\right\}.$$

b) $a_3 < 0 < a_1, a_2$, in which case (B.1) returns

$$P_{Gap} = \mathbb{P}\left(-\frac{\varepsilon_2}{a_2} < \delta Z(t) < \min\left\{-\frac{\varepsilon_1}{a_1}, -\frac{\varepsilon_3}{|a_3|}\right\}\right),$$

which is non-zero for

$$\varepsilon_2 > -a_2 \min\left\{-\frac{\varepsilon_1}{a_1}, -\frac{\varepsilon_3}{|a_3|}\right\}.$$

c) $a_1 < 0 < a_2, a_3$; then, it follows from (B.1)

$$P_{Gap} = \mathbb{P}\left(\delta Z(t) > \max\left\{\frac{\varepsilon_1}{|a_1|}, \frac{\varepsilon_3}{a_3}\right\}\right),$$

d) $a_2, a_3 < 0 < a_1$; then (B.1) implies

$$P_{Gap} = \mathbb{P}\left(\delta Z(t) < \min\left\{-\frac{\varepsilon_1}{a_1}, -\frac{\varepsilon_3}{|a_3|}\right\}\right).$$

C Uncollateralized Exposure

In the case of a single swap contract, the following holds.

Corollary 5 *If $B = C = D = 0$, $E \downarrow -\infty$, $F \uparrow \infty$, the market consistent value of the uncollateralized exposure of a swap with value function given by (11) reduces to*

$$\alpha_3(t)\beta(t; a_3 Z)\mathbb{E}_Z\left(e^{-rt}\left(S_3(0)e^{(r-q_3-\varphi_{Y_3}(-i))t+Y_3(t)} - \tilde{K}\right)^+\right)$$

for

$$\tilde{K} = \frac{A\bar{K}_3(t)}{\alpha_3(t)\beta(t; a_3 Z)}.$$

The result follows from Proposition 1 by setting the parameters accordingly and the properties of the conditional expectation

In the case of the portfolio of swap, we obtain.

Corollary 6 *If $B = C = D = 0$, $E \downarrow -\infty$, $F \uparrow \infty$, the market consistent value of the uncollateralized exposure of a portfolio $\Pi(t)$ of swaps with value function given by (11) reduces to*

$$Ae^{-rt}\left[\sigma_1 \frac{1}{\sqrt{2\pi}} e^{-\left(\frac{m_1}{\sigma_1}\right)^2} + m_1 \mathcal{N}\left(\frac{m_1}{\sigma_1}\right) + \sum_{\alpha_1=3}^{4} \frac{1}{\alpha_1!} \frac{K_{\Pi(t)}^{\alpha_1}}{\sigma_1^{\alpha_1}} \sum_{i=0}^{\alpha_1} h_i^{\alpha_1} \left(\sigma_1 \bar{m}_{i+1} + m_1 \bar{m}_i\right)\right],$$

for

$$\begin{aligned} \bar{m}_k &= (k-1)\bar{m}_{k-2} + \left(-\frac{m_1}{\sigma_1}\right)^{k-1} \frac{1}{\sqrt{2\pi}} e^{-\frac{\left(\frac{m_1}{\sigma_1}\right)^2}{2}}, \\ \bar{m}_0 &= \mathcal{N}\left(\frac{m_1}{\sigma_1}\right), \qquad \bar{m}_{-1} = 0. \end{aligned}$$

$\mathcal{N}(\cdot)$ denotes the standard normal cumulative distribution function, and $h_i^{\alpha_1}$ denotes the i coefficient of the terms in the 1-dimensional Hermite polynomial of order α_1.

The intuition behind the proof is that the marginal density of a bivariate Gram-Charlier A density is still Gram-Charlier A (see Mardia, 1970, for further details). Thus, when integrating the result of Proposition 2 along the y dimension, we need to set $\alpha_2 = 0$ and $j = 0$. The rest of the argument follows from the properties of the bivariate normal distribution.

Finally, for the case of a large, equally weighted and homogeneous portfolio of swaps, we obtain.

Corollary 7 *If $B = C = D = 0$, $E \downarrow -\infty$, $F \uparrow \infty$, the market consistent value of the uncollateralized exposure of a large, equally weighted and homogeneous portfolio of swaps with value function given by (11) reduces to*

$$Ae^{-rt}\left[\sigma_1 \frac{1}{\sqrt{2\pi}} e^{-\left(\frac{m_1}{\sigma_1}\right)^2} + m_1 \mathcal{N}\left(\frac{m_1}{\sigma_1}\right)\right] + o(n^{-1/2}).$$

The argument follows by taking the limit. We note the Bachelier price structure of the option value.

D Calibration: the parameter set of the factor model

For the case of three assets, constraint (21) can be solved analytically. Let c_{ij} denote the observed covariance between asset i and asset j. Then

$$\begin{aligned} a_1 &= sign\left(\frac{c_{12}}{c_{23}}\right)\sqrt{\frac{|c_{12}c_{13}|}{|c_{23}|\mathbb{V}ar(Z(1))}}, \\ a_2 &= sign\left(c_{23}\right)\sqrt{\frac{|c_{12}c_{23}|}{|c_{13}|\mathbb{V}ar(Z(1))}}, \\ a_3 &= sign\left(\frac{c_{13}c_{23}}{c_{12}}\right)\sqrt{\frac{|c_{13}c_{23}|}{|c_{12|}\mathbb{V}ar(Z(1))}}. \end{aligned}$$

Note: if the sample correlation ρ_{ij} is used instead, this can be converted using the parameters of the margin processes obtained in step 1 of the calibration procedure described in Section 5.1 .

The recovery of the parameters of the idiosyncratic components from the two-step procedure described in Section 5.1 for the case of the NIG process can be obtained in analytical form. Let us assume that each idiosyncratic component Y_j, $j = 1, 2, 3$, is NIG with parameters $(\beta_j, \gamma_j, \nu_j)$. For a given set of parameters for the margin process X_j, the systematic process Z and the loading factors, let us denote $\bar{K}_{Y_j}^{(\alpha)} = K_{X_j}^{(\alpha)} - a_j^{\alpha} K_Z^{(\alpha)}$ the 'implied' cumulant of order α of the systematic component Y_j. Then the solution to the cumulant condition (22) is

$$\begin{aligned} \beta &= \frac{3(\bar{K}_Y^{(2)})^2 \bar{K}_Y^{(3)}}{3\bar{K}_Y^{(2)}\bar{K}_Y^{(4)} - 4(\bar{K}_Y^{(3)})^2}, \\ \gamma^2 &= \frac{\bar{K}_Y^{(2)}(3\bar{K}_Y^{(2)}\bar{K}_Y^{(4)} - 5(\bar{K}_Y^{(3)})^2)}{3\bar{K}_Y^{(2)}\bar{K}_Y^{(4)} - 4(\bar{K}_Y^{(3)})^2}, \\ \nu &= \frac{3\bar{K}_Y^{(2)}\bar{K}_Y^{(4)} - 4(\bar{K}_Y^{(3)})^2}{9(\bar{K}_Y^2)^{(3)}} \end{aligned}$$

(we have omitted the dependence on the component index j).

E Further results

Figure E.1 illustrates, as second example, the CVA profile of a Forward contract written on the same index as the Swap considered in this paper, entered by the same counterparties.

We note the same sensitivity of the forward CVA versus right-way risk and wrong-way risk. Further, although the forward can be considered as a special case of the swap - as discussed in Section 3.3 - the two contracts generate different profile shapes due to their different payment schedule. The forward contract, in fact, is settled at maturity only, meaning that the credit risk exposure for the investor increases the further in the future we look ('diffusion' effect).

In Table E.1, we report the results of a sensitivity analysis of the CVA to different collateral agreements and initial margin on the CVA. Panel (a) reports the uncollateralized CVA under the assumption of no initial margin in correspondence of different scenarios of right/wrong-way risk. These are the benchmark values. In panel (b) we report the impact of the given collateral schemes on the CVA, computed as the (percentage) difference between the collateralized CVA and the corresponding uncollateralized one. In details, schemes 1 - 3 concern unilateral agreements for different values of the triggering threshold H_1. As expected, the mitigation of

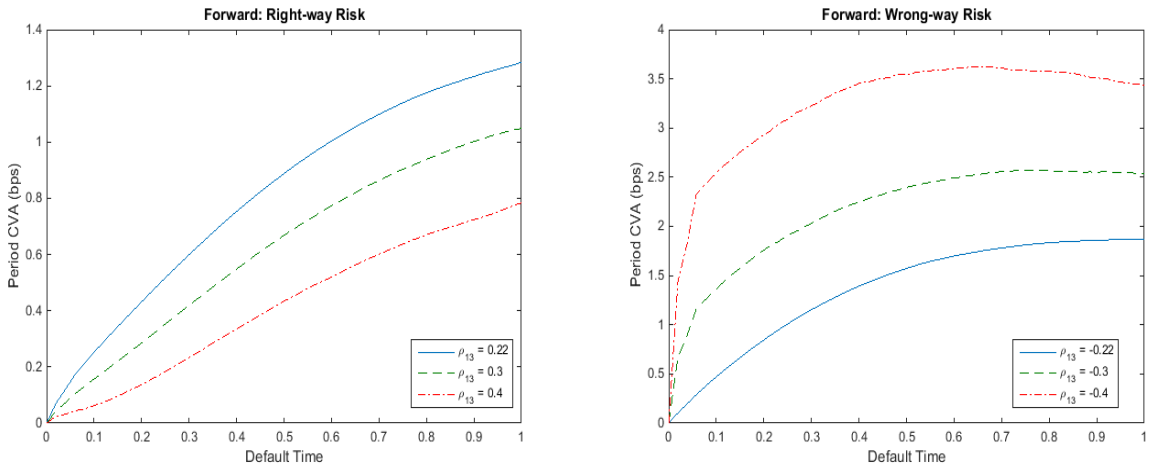

Figure E.1: Uncollateralized CVA - Right-way Risk and Wrong-way Risk. Forward contract. Parameter set: Table 3. Other parameters: $S_1(0) = S_2(0) = S_3(0) = 1$, $T = 1$ year, $r = 0.45\%$. Weekly default monitoring. MC+Hilbert: 10^6 simulation trials, 2^{10} grid points. COS: 2^9 grid points, $L = 15$.

the CVA due to the collateral posted in the investor's favour is milder the higher H_1 regardless of right/wrong-way risk. A higher value of H_1, in fact, originates both a smaller probability of the collateral being called and a smaller collateral amount itself. Schemes 4 - 8 illustrate the case of bilateral agreements: in schemes 4 - 6 the triggering threshold for the investor, H_2, is fixed at the tightest possible level, whilst the counterparty threshold H_1 is allowed to vary; in schemes 6 - 8 instead we relax the investor threshold H_2, keeping H_1 fixed. In all cases, the CVA reduces compared to the uncollateralized case, but less in presence of bilateral schemes compared to the unilateral ones. This is due to the increased credit exposure generated by the requirement on the investor to post collateral. The milder H_2 (i.e. the greater H_2 is in absolute value), the less stringent the requirement. Further, we notice that the collateral agreements are particularly effective in presence of right-way risk. Wrong-way risk on the other hand reduces the effectiveness of the collateralization as, when $\rho_{13} < 0$, increases in the value of S_3 are more likely to be associated with a worsening of the counterparty probability of default, which counteracts the mitigation effect offered by the collateral posting in the investor's favour. Table E.1 also shows the effect of a minimum transfer amount $M > 0$ (schemes 9 - 11 in panel b): as this provision makes the posting thresholds less binding, the CVA increases.

Table E.1, panel (c) shows the percentage impact of the initial margin on both uncollateralized and collateralized CVA, in correspondence of all schemes considered in panel (b). We observe the very strong 'smoothing' effect of the initial margin on CVA regardless of the correlation scenario and the collateral scheme in place. Indeed the initial margin manages to mitigate a large percentage of the residual risk either left by soft collateral triggering thresholds, or generated by situations of strong wrong-way risk.

				a) Uncollateralized CVA (bps)					
				Right-way Risk			Wrong-way Risk		
	scenario: s			1	2	3	4	5	6
	CVA (bps)			820.2608	600.4706	368.9231	1458.0926	2590.5305	4119.8749
	95% C.I.			819.8556	599.8578	368.0877	1455.6966	2581.9565	4105.7774
				820.6660	601.0834	369.7585	1460.4887	2599.1046	4133.9723
Collateral scheme									
	H_1	H_2	M	b) Collateral agreement impact					
1	0	-	0	-89.92%	-90.70%	-91.76%	-80.16%	-59.64%	-46.60%
2	0.25	-	0	-85.40%	-86.94%	-89.17%	-74.89%	-55.19%	-42.76%
3	1	-	0	-67.09%	-70.68%	-76.04%	-57.16%	-41.99%	-32.22%
4	0	0	0	-78.05%	-77.13%	-76.75%	-66.76%	-44.89%	-31.84%
5	0.25	0	0	-73.60%	-73.42%	-74.19%	-61.50%	-40.50%	-27.96%
6	1	0	0	-54.64%	-56.67%	-60.71%	-43.31%	-27.18%	-17.41%
7	1	-1	0	-65.39%	-68.71%	-73.64%	-54.00%	-36.42%	-25.50%
8	1	-2	0	-66.43%	-70.00%	-75.20%	-56.17%	-39.81%	-29.29%
9	1	-	1	-62.61%	-66.15%	-70.94%	-53.34%	-39.42%	-30.30%
10	1	0	1	-51.77%	-53.77%	-57.43%	-41.85%	-26.66%	-17.36%
11	1	-1	1	-60.53%	-63.75%	-68.24%	-50.55%	-34.52%	-24.45%
	H_1	H_2	M	c) Initial Margin and Collateral agreement impact					
No Collateral				-77.64%	-78.2%	-80.89%	-71.14%	-64.61%	-57.64%
1	0	-	0	-99.51%	-99.52%	-99.53%	-98.89%	-93.34%	-86.50%
2	0.25	-	0	-99.47%	-99.48%	-99.51%	-98.7%	-92.76%	-85.69%
3	1	-	0	-99.11%	-99.12%	-99.2%	-97.27%	-89.52%	-81.38%
4	0	0	0	-98.41%	-97.94%	-97.08%	-97.24%	-88.72%	-79.64%
5	0.25	0	0	-98.35%	-97.88%	-97.02%	-96.96%	-87.78%	-78.28%
6	1	0	0	-97.98%	-97.51%	-96.71%	-95.53%	-84.54%	-73.97%
7	1	-1	0	-99.00%	-98.98%	-99.01%	-97.1%	-88.27%	-78.86%
8	1	-2	0	-99.07%	-99.07%	-99.13%	-97.24%	-89.26%	-80.62%
9	1	-	1	-98.46%	-98.46%	-98.64%	-96.21%	-88.32%	-80.11%
10	1	0	1	-97.83%	-97.58%	-97.37%	-94.96%	-84.2%	-73.77%
11	1	-1	1	-98.37%	-98.34%	-98.46%	-96.07%	-87.28%	-77.96%

Table E.1: CVA & Right-Way/Wrong-Way Risk. Panel (a): uncollateralized CVA (in bps) and 95% Confidence Interval. Right-Way Risk Scenarios - $s = 1$: $\rho_{13} = 0.2151$ (benchmark); $s = 2$: $\rho_{13} = 0.3$; $s = 3$: $\rho_{13} = 0.4$. Wrong-Way Risk Scenarios - $s = 4$: $\rho_{13} = -0.2151$ (benchmark); $s = 5$: $\rho_{13} = -0.3$; $s = 6$: $\rho_{13} = -0.4$. Other correlations: Table 3. Other parameters: $S_1(0) = S_2(0) = S_3(0) = 1$, $T = 1$ year. Weekly monitoring. Panel $(b) - (c)$: collateralized CVA without/with IM. H_1: counterparty agreement threshold; H_2: investor agreement threshold; M: minimum transfer amount. Impact of collateral and IM agreements computed as $(Coll.CVA_s - Uncoll.CVA_s)/Uncoll.CVA_s$ or $((Coll. + IM)CVA_s - Uncoll.CVA_s)/Uncoll.CVA_s$. Schemes 1-3: unilateral collateral agreement. Schemes 4-12: bilateral collateral agreement. Schemes 9-11: collateral with MTA. MC+Hilbert: 10^6 simulation trials, 2^9 grid points. COS: 2^9 grid points, $L = 15$.